

NARROW BEAM ECHO SOUNDS

William C. Pfingstag

LIBRARY
NAVAL POSTGRADUATE SCHOOL
MONTEREY, CALIF. 93940

NARROW-BEAM ECHO SOUNDING

by

William C. Pfingstag

//

Lieutenant Commander, United States Navy

S.B., United States Naval Academy
(1962)

SUBMITTED IN PARTIAL FULFILLMENT
OF THE REQUIREMENTS FOR THE
MASTER OF SCIENCE DEGREE IN ELECTRICAL ENGINEERING
AND THE PROFESSIONAL DEGREE, NAVAL ENGINEER

at the

MASSACHUSETTS INSTITUTE OF
TECHNOLOGY

June, 1971

NARROW BEAM ECHO SOUNDING

by

William C. Pfingstag

Lieutenant Commander, United States Navy

Submitted to the Department of Electrical Engineering and to the Department of Naval Architecture and Marine Engineering in partial fulfillment of the requirements for the degree of Master of Science in Electrical Engineering and the Professional Degree, Naval Engineer.

ABSTRACT

Narrow beam echo sounders are examined for their use as a tool to obtain more refined data concerning ocean bottom topography. A five foot line hydrophone array is examined in some detail including theoretical and at sea data collection. Theoretical predictions of the major lobe of the beam pattern correlates reasonably well with test results and a narrow, near conical beam can be obtained from line arrays by signal processing and proper physical orientation.

The problems of echograph interpretation are examined and some solutions given. Simple examples describing the computation of actual bottom depth and slope as a function of recorded depth, transducer aperture angle and echo length are discussed.

The effects of refraction are found to be significantly reduced through the use of a narrow cone angle.

In addition to the normal echograph, it is suggested that via a simple mathematical electronic circuit, three additional bits of data could be presented to the at sea oceanographer to aid him in assessing ocean bottom topography.

Thesis Supervisor: Harold E. Edgerton
Title: Institute Professor, Emeritus

ACKNOWLEDGEMENTS

The advice and encouragement of many people contributed to this study. In particular the author wishes to thank the following persons:

Dr. Harold E. Edgerton for the inspiration and enthusiasum that he provided as my thesis supervisor.

Dr. Ira Dyer who provided my first formal introduction to the world of oceanography and underwater sound, and continued with the unenviable job of supplying technical advice and constructive criticism.

Mr. William O. Rainnie and the members of the DSRVG who provied the opportunity and assistance for some practical work in underwater sound.

Mr. Pete DeEntremont and the group at the Sonar Test Barge of the Boston Naval Shipyard for their patience and assistance in obtaining much of the experimental data.

TABLE OF CONTENTS

	<u>PAGE</u>
TITLE PAGE	1
ABSTRACT	2
ACKNOWLEDGEMENTS	3
TABLE OF CONTENTS	4
LIST OF FIGURES	5
LIST OF TABLES	7
CHAPTER I	INTRODUCTION 8
CHAPTER II	EXAMPLES OF NARROW BEAM ECHO SOUNDERS 13
CHAPTER III	EXPERIMENTAL RESULTS 20
CHAPTER IV	INTERPRETATION OF ECHOGRAMS 33
CHAPTER V	EFFECTS OF REFRACTION AND VELOCITY PROFILE 41
CHAPTER VI	CONCLUSIONS 44
CHAPTER VII	RECOMMENDATIONS 47
BIBLIOGRAPHY	51
APPENDIX	A. Analytical Development for Computer Program 53
	B. Computer Program 55
	C. Examples of Schuler's Method 56
	D. Signal Processor 61
	E. JT Hydrophone Data 62
	F. EDO Model 202 Transducer 63

LIST OF FIGURES

<u>FIGURE</u>	<u>TITLE</u>	<u>PAGE</u>
1	Resolution Geometry	11
2	Line Hydrophone Array Geometry	15
3	Computed Beam Pattern for Shaded Ten Element Line Array	17
4	Computed Beam Pattern for Crossed Array	18
5	Sonar Test System Block Diagram	19
6	"V" Hydrophone in yz Plane	21
7	"T" Hydrophone in yz Plane	22
8	"V" Hydrophone in xz Plane	23
9	"T" Hydrophone in xz Plane	24
10	"V·T" Multiply yz Plane	25
11	"V&T" Add yz Plane	26
12	Beam Patterns on Sea Bottom	28
13	Lone Rock/Quicks Hole - UQN-1	29
14	Lone Rock/Quicks Hole - "V" Phone	30
15	Lone Rock/Quicks Hole - "T" Phone	31
16	C.&G.S. #263 - Lone Rock/Quicks Hole	32
17	Bottom Slope - Dual Recording	37
18	Depth Correction for Ships Speed	38
19	Assumed Sound Velocity Profile	41
20	Time/Sound Path Models	42
21	Bottom Slope - Instantaneous/ Time Average $0 < \theta < \beta$	49
22	Bottom Slope - Instantaneous/ Time Average $\beta < \theta < 90 - \beta$	50

23	Echo Length - Flat Bottom	56
24	Echo Length - Flat/Slope Transition	57
25	Echo Length - Shallow Slope	58
26	Echo Length - Steep Slope	59

LIST OF TABLES

<u>TABLE</u>	<u>TITLE</u>	<u>PAGE</u>
1	Resolution Data	11
2	Echo Length Timing Errors	43
3	Depth - Echo Length - Bottom Slope	60

CHAPTER I

INTRODUCTION

HISTORY

Ancient records indicate that the earliest soundings were made by the Egyptians sometime around 2000 B.C. via the use of a sounding lead. This system was also used by the ancient Greeks and the measurement of the Nile is mentioned by Herodotus. The lead line concept remained essentially unchanged until the 1800's. The British Royal Navy and the American Navy were fairly active in the 18th and 19th centuries with a cannon ball and a reel of strong twine used for making deep soundings. These soundings were generally in error due to currents, ship motion, and the inability to tell when the cannon ball reached bottom. The use of sound, in particular the measurement of the time that it takes for sound to go from the surface to the bottom and back, was suggested by C. Bonnycastle in 1838.⁽⁴⁾ Most early experiments were unsuccessful and instead the lead line continued to be used. In 1875, Lord Kelvin developed a pressure sensing tube which was later modified to record the maximum pressure attained. Other modifications were made to the Kelvin tube and in 1912, under the name of Rude-Fisher tube, it became the standard instrument used by the Coast and Geodetic Department for sounding shoal depths. For deep soundings a heavy weight and a reel of

piano wire were used. Between 1910 and 1920 the use of sound as a depth measuring method was shown to be practical. In Europe, A. Behm was able to obtain echoes from the sea bottom. He is also credited with solving the problem of determining short time intervals and was able to manufacture an acoustical sounding machine in 1919.⁽⁴⁾ Around this same time period, Professor Fessenden developed an electromagnetic oscillator that could produce a continuous series of undamped waves. The Fessenden Oscillator could be used both as a transmitting device and a receiver. This device was successfully tested in Massachusetts Bay in 1914 on board the Coast Guard Cutter MIAMI.⁽⁵⁾ With the development of the vacuum tube and a short pulse oscillator, it became possible for the installation of a commercial depth sounder in 1924.⁽⁵⁾

WHY NARROW BEAM ECHO SOUNDER?

Today's commercial depth sounders have not progressed much beyond their original capabilities. Most refinement has been in the area of electronics. Present commercial depth sounders generally have the following specifications:

Frequency: 3.5-160 kHz with 12 kHz standard
Transmit Power: 100-800 watts peak power @ 1%
duty cycle
Transducer Beam Width: 40°-60°
Sweep Scales: 5-2000 fms
Source Level: 80-115 dB re 1 μ b @ 1yd
Cost: \$5,000-\$15,000

The wide angle echo sounder is very adequate for surface ship navigation, but when used on a surface ship to acquire data for submersible operations, it will not provide the detail required for safe submersible navigation near the bottom. This lack of precise knowledge of bottom topography presents a significant hazard to deep submersibles. On the edge of the Continental Shelf, where much exploration and investigation is being done, there exists rugged topography that cannot be accurately determined by wide angle transducers. The cliffs and canyons that exist are difficult if not impossible to determine from a wide angle echogram. Figure (1) and Table (1) give comparative resolution data. Present-day echo sounders ($2\beta \approx 60^\circ$) are seen to be unable to resolve horizontal scales of 1,000 feet or more; such scales are large compared to the size and positional accuracy of submersibles. Several incidents have occurred to submersibles that might have been avoided had better bottom data been available. The objective, then, is that through a careful, high resolution survey of a dive site and proper interpretation of the echograms, a fairly detailed picture of the bottom be obtained.

There have been some efforts to improve resolution by reducing beamwidth. The British and Germans have done work in this area, with the National Ocean Survey, formerly the Coast and Geodetic Survey, being one of

RESOLUTION GEOMETRY

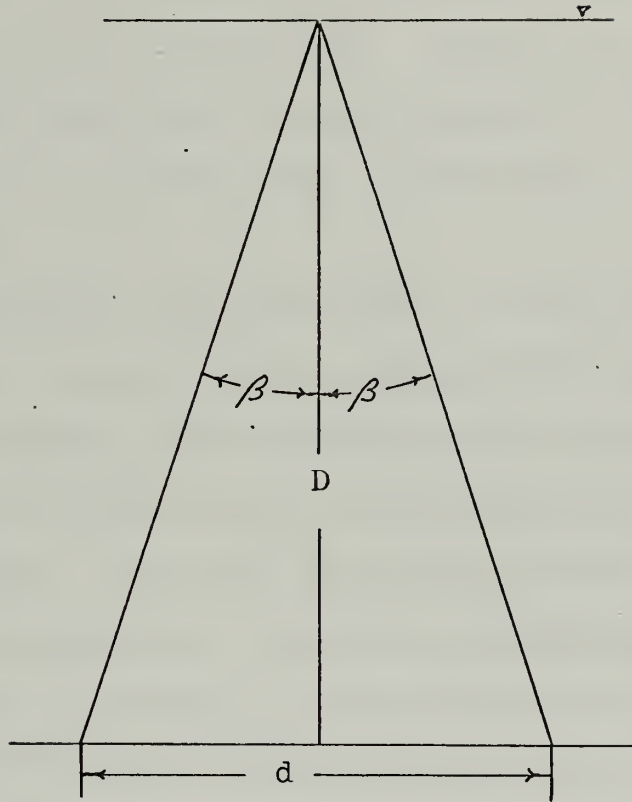


FIGURE 1

RESOLUTION DATA

$$d = 2D \tan \beta$$

$\beta \backslash D$	6000'	3000'	1000'
5°	1045'	524'	174'
1 1/3°	261'	131'	43'
30°	6950'	3470'	1150'

TABLE 1

the leading investigators in this country. Beamwidth is generally reduced by making a larger transducer or increasing frequency. The higher the frequency, however, the smaller the depth capability. Through electronic means, the National Ocean Survey presently have a pitch and roll stabilized beam only $2\frac{2}{3}^{\circ}$ wide useable to 6000 fms.

Research is presently being conducted in the field of parametric sonar. A narrow beam is obtained through the use of a high frequency beam (near 200 kHz) and by making use of the non-linear nature of traveling waves in an absorbing medium. By having two closely spaced high frequency, high amplitude, interacting sound waves, an appreciable amount of energy at the difference frequency is produced.⁽¹⁴⁾ Thus one can obtain a directive low frequency narrow beam, but at the expense of high power levels.

CHAPTER II

EXAMPLES OF NARROW BEAM ECHO SOUNDERS

GENERAL

Two specific hydrophones will be examined as examples of narrow beam transducers. A line hydrophone (U.S. Navy "DT 70/BQR 3A/JT") will be described in detail using both theoretical and experimental methods. Two line hydrophones will be combined and the beam patterns examined. A narrow beam circular array will be presented as a simple, small unit that may provide a reasonable solution to obtaining a narrow symmetric beam pattern.

THEORETICAL

For linear two dimensional arrays of equally spaced, equally sensitive elements, the width of the major lobe will depend upon the number of elements and upon the length of the array in wave lengths (L/λ). The greater the number of elements or the higher the operating frequency, the narrower the main lobe. The Directivity Index, which is a measure of beam width, is given by $D.I. = 10 \log \frac{n}{1 + \frac{2}{n} \sum_{e=1}^{n-1} \frac{(n-e) \sin(2\pi e d/\lambda)}{2\pi e d/\lambda}}$ (23)

where n is the number of elements

and d is element spacing

This reduces to $10 \log \frac{2L}{\lambda}$ for a continuous line of length L if $L \gg \lambda$. The number and amplitude of side

lobes depends upon L/λ and element spacing. Side lobe amplitude reduction can be obtained by varying the sensitivity of the elements; however, this will tend to widen the main lobe.

The theoretical computations of beam patterns were for a linear array of elements each of finite length as developed by Tucker and Gazey.⁽²⁰⁾ The analytical details of this computation as utilized in a computer program are summarized in Appendix (A). The computer program as such is described in Appendix (B).

The input data required for the computer program is:

- 1) frequency
- 2) element shading factors

Assumptions concerning the computations were:

- 1) a five foot line array of ten finite elements with element length of 5.75 inches and an element separation of 5.85 inches was used as representative of a "JT" hydrophone
- 2) each element was considered to be a uniform line array (ie. sensitivity of $1/a$, where "a" is element length)
- 3) the beam pattern in the plane perpendicular to the hydrophone axis is assumed to be uniform

In order to obtain some representation of pattern shape on the sea floor, skew angles were introduced as described in Figure (2).

LINE HYDROPHONE ARRAY GEOMETRY

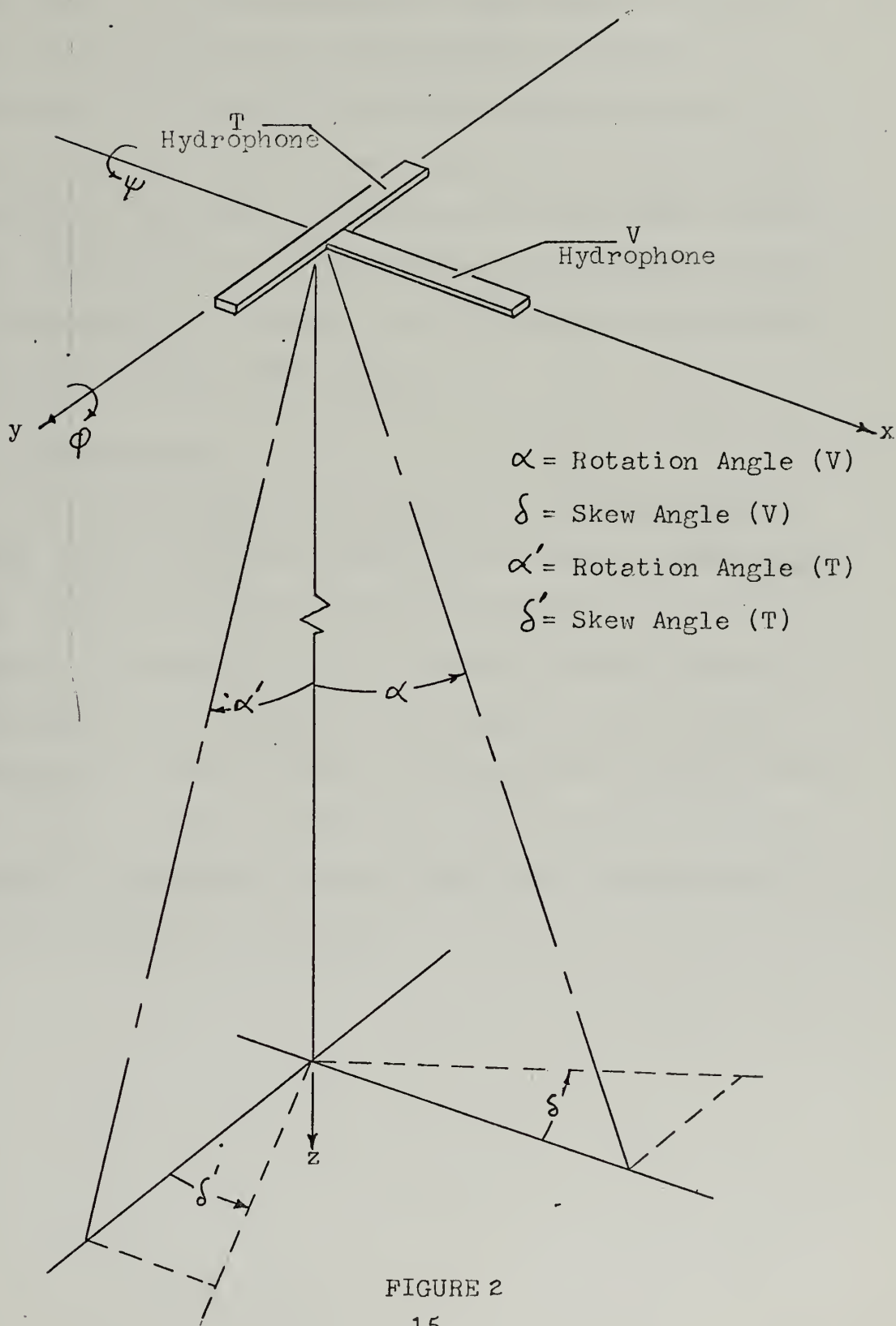
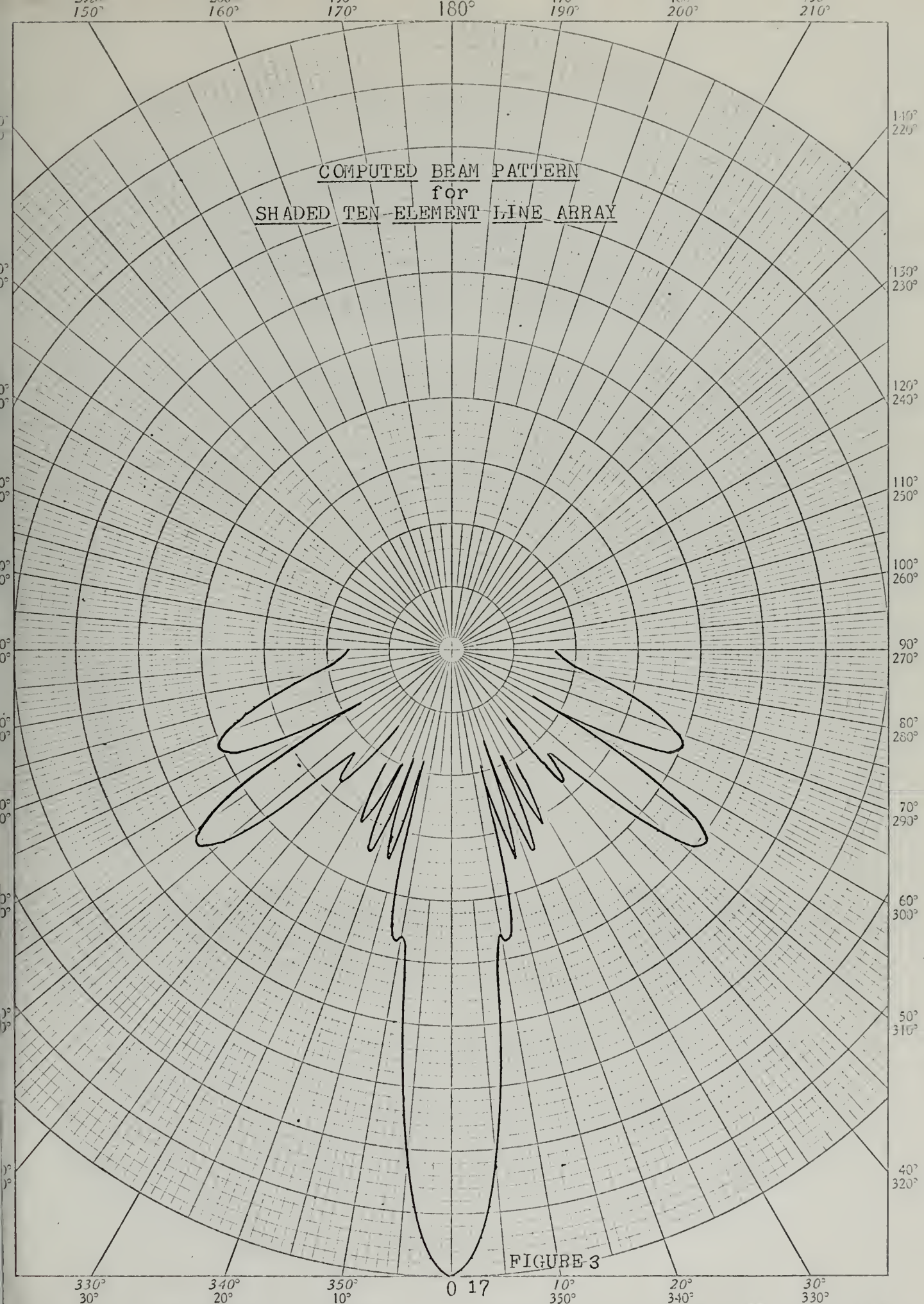


FIGURE 2

The computer output was, for each skew angle selected, the rotation angle verses beam pattern (dB). The values for beam pattern were normalized to zero at zero rotation angle and are described in Figure (3). The signals from two perpendicular hydrophones can be combined to give various beam patterns, a fairly common practice in the field of communication and radio astronomy. Figure (4) is a graph showing the computed results of multiplying the signals from two perpendicular hydrophones for various skew angles.

EXPERIMENTAL

The experimental investigation was partially conducted at the Sonar Test Barge at the Boston Naval Shipyard. The set-up used consisted basically of an active projector located on the line array's acoustic axis at a distance of 17.7 yards. The Fresnel range for this projector is about 15 feet. The array was rotated and a polar beam pattern automatically computed and plotted. Figure (5) describes the electronic test hook-up used. At sea tests were also made.



COMPUTED BEAM PATTERNS
for
CROSSED ARRAY

Signal Processing - Multiply

Skew Angles (δ) - $10^\circ, 20^\circ, 45^\circ, 70^\circ, 80^\circ$

NOTE: For rotation angles greater
than 20° , beam patterns remain
below 35dB down.

$20^\circ/70^\circ$

45°

$10^\circ/80^\circ$

FIGURE 4

330°
 30°

340°
 20°

350°
 10°

0 18

10°
 350°

20°
 340°

30°
 330°

SONAR TEST SYSTEM BLOCK DIAGRAM

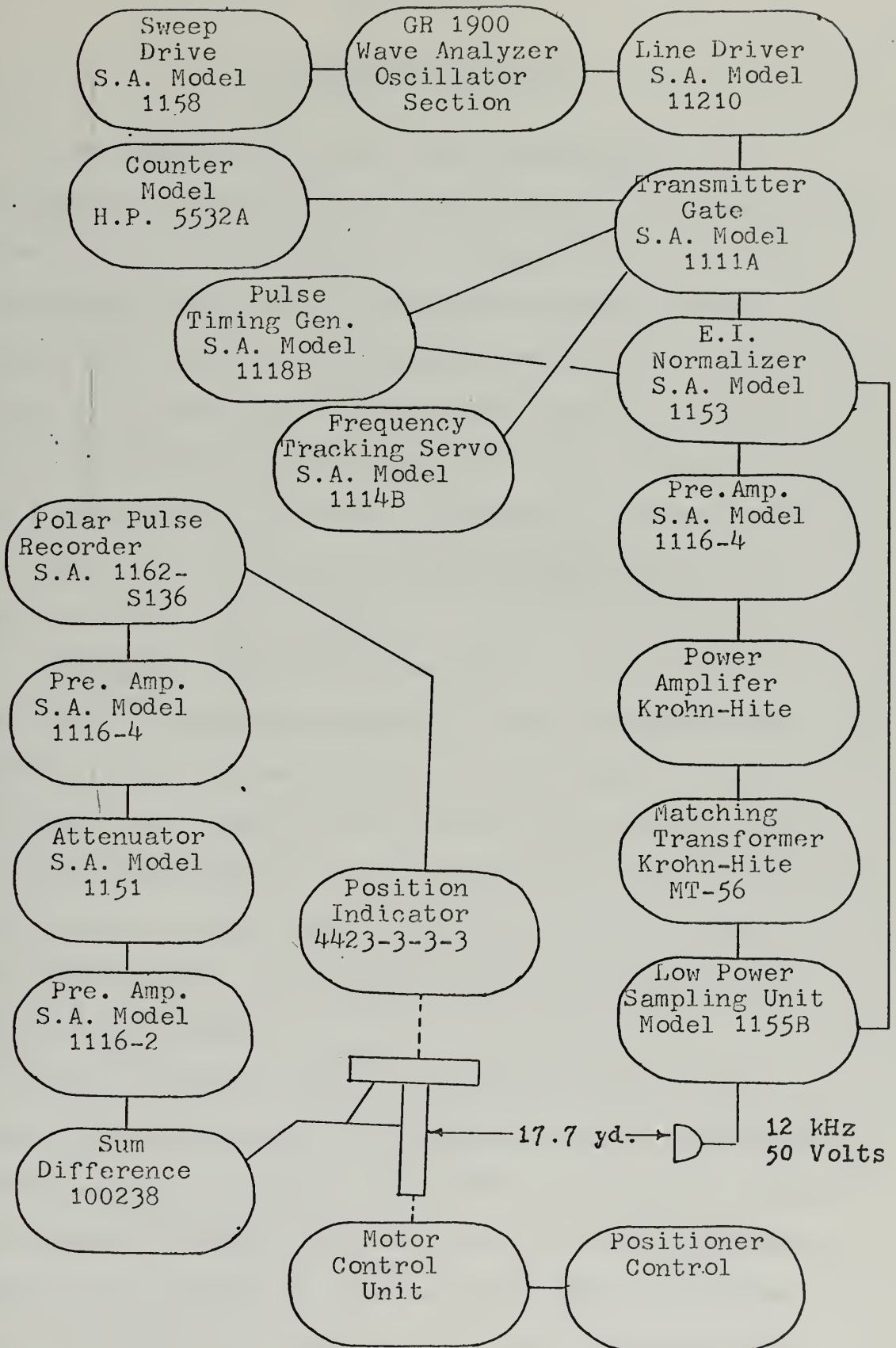


FIGURE 5
19

CHAPTER III

EXPERIMENTAL RESULTS

Beam patterns for the V and T hydrophones, as described in Figure (2), rotated in the ψ direction are shown in Figures (6) and (7). Patterns for the V and T hydrophones rotated in the ϕ direction are shown in Figures (8) and (9). The pattern for the V hydrophone in the 'xz' plane does not represent the true pattern since the array was not rotated about the midpoint of the V hydrophone, but rather at a point 8 inches from its midpoint. This would account for the widening of the main beam.

The signal processor, described in Appendix (D), was used to combine the signals of the two hydrophones and the results of multiplying the two signals is shown in Figure (10). Due to limitations in the preamplifiers and the characteristics of the multiplier, the multiply beam pattern quickly goes into noise. Pre-filtering of the input signals was attempted, but noise (internal) was still a problem.

Multiplying the input signals from the two hydrophones was investigated for it gives a fairly symmetrical, narrow pattern on the sea floor.⁽²²⁾ A process of adding was examined, Figure (11), but since the relative phasing between the elements of the two hydrophones is unknown and not optimum, the theoretically possible narrow pat-

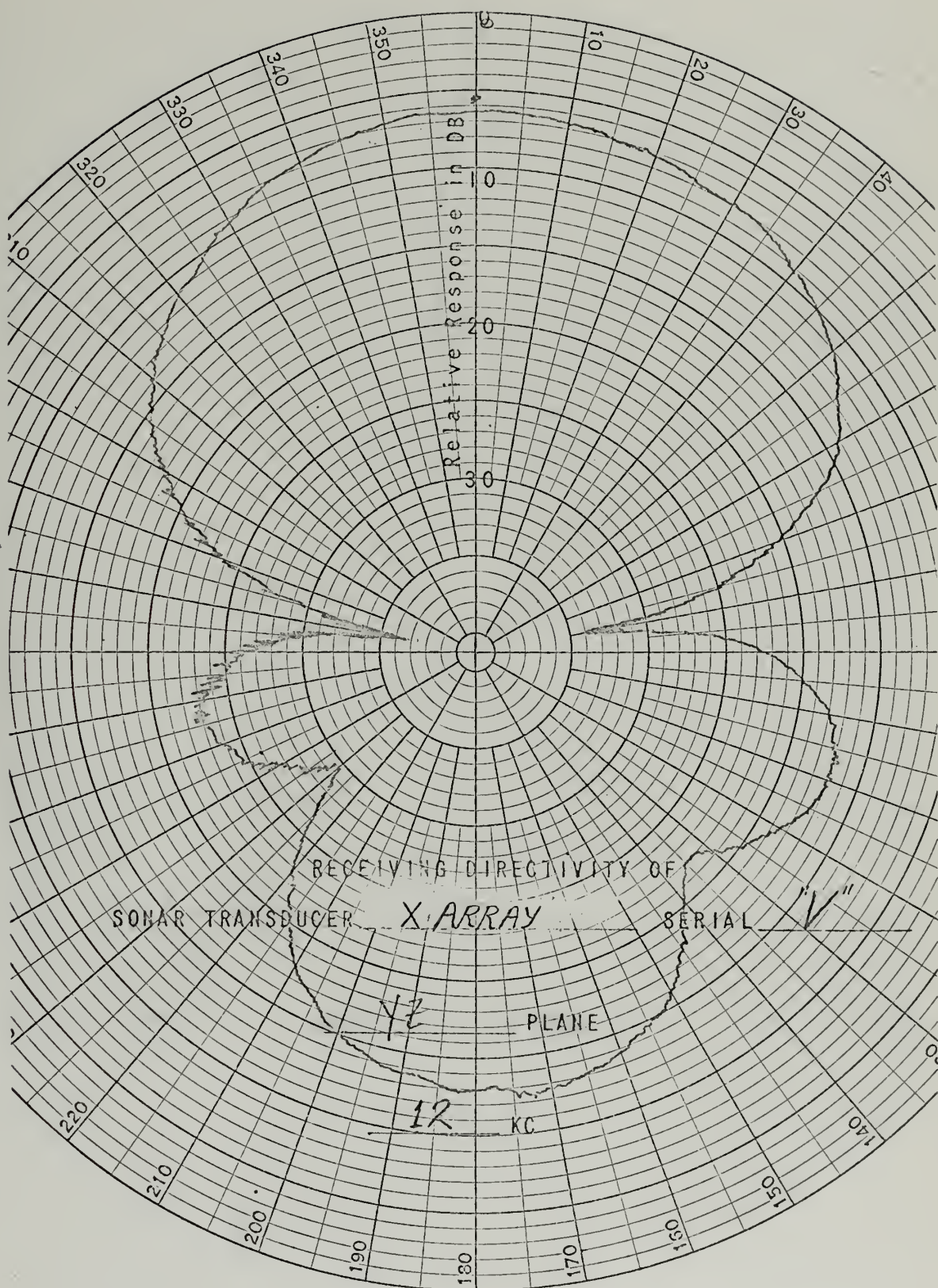


FIGURE (6)
21

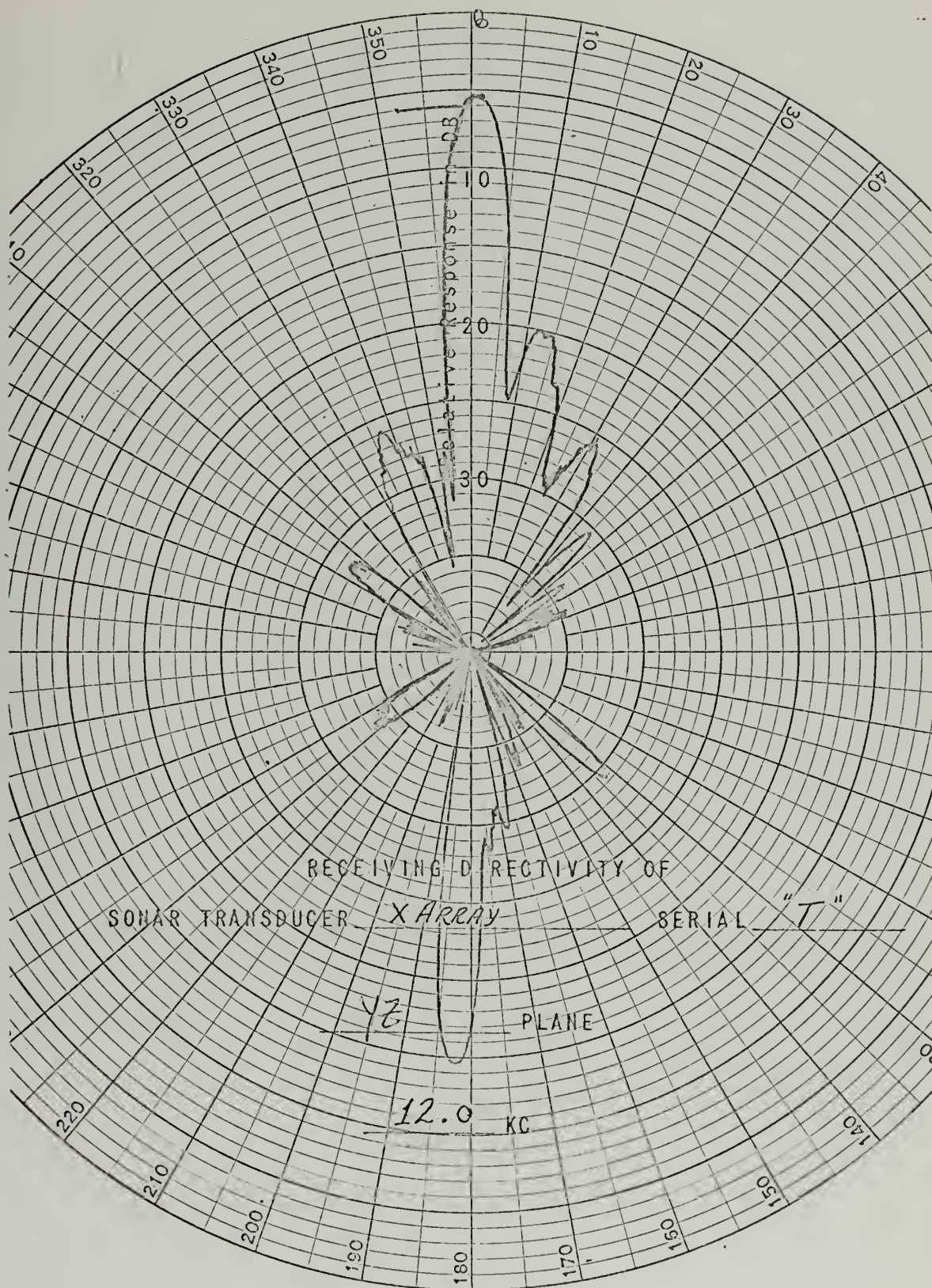


FIGURE (7)

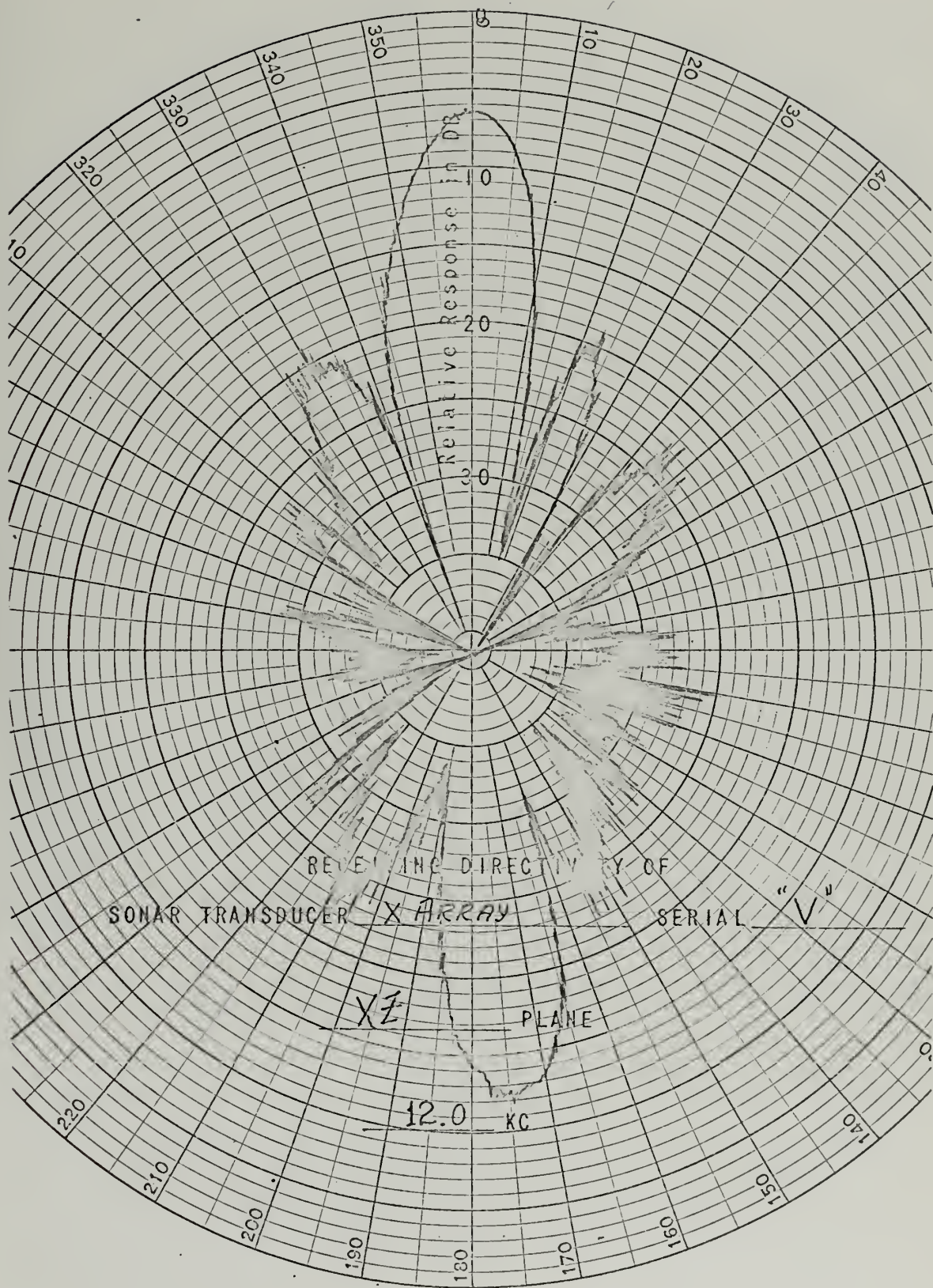


FIGURE (8)
23

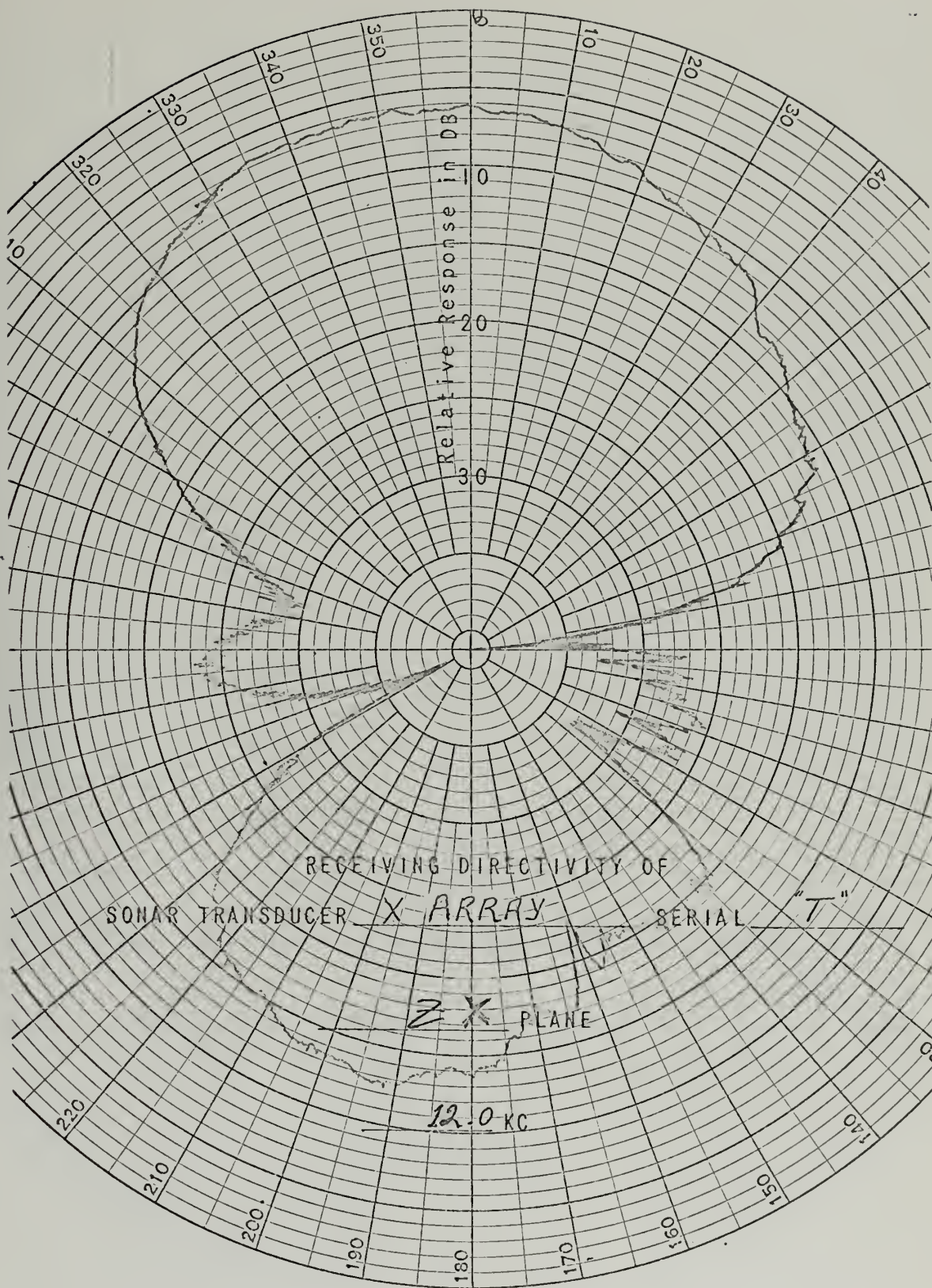


FIGURE (9)
24

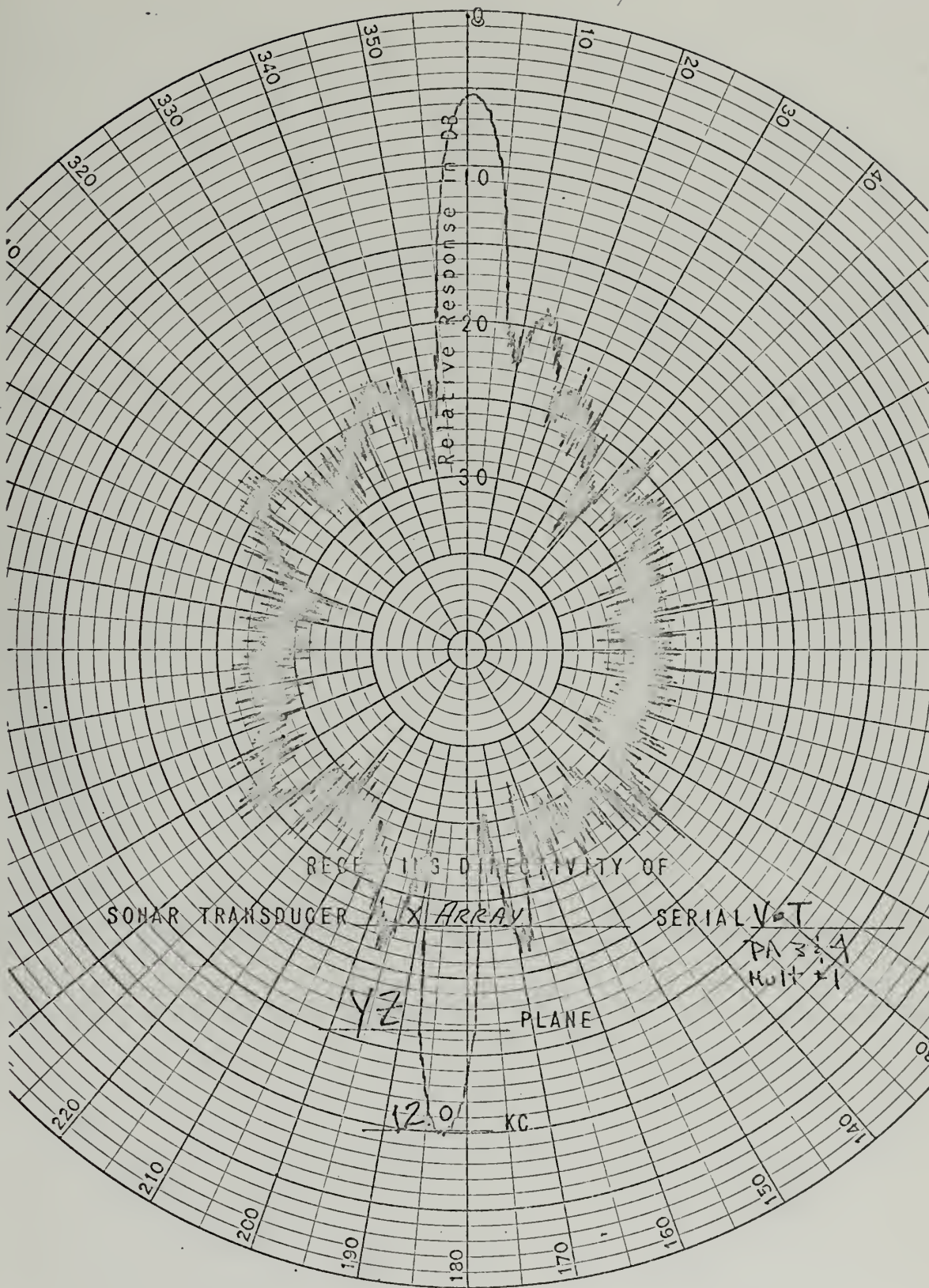


FIGURE (10)

tern was not obtained. Figure (12) compares the sea floor pattern of a single line and the multiplied pattern.

The line array was taken to sea mounted on the bottom of the starboard hull of RV LULU and some shallow water results were obtained over an area known as Lone Rock/Quicks Hole. Recordings were made using an EDO UQN-1 wide angle transmitter and the line array; simultaneously, standard echographs were obtained with a OSR-119T recorder that was part of the overall UQN-1 system. Magnetic recordings were made for each line array and from these tapes echographs shown in Figures (14) and (15) were made. An operating frequency of 12kHz was used. Using the first arrival, the slopes in the direction of travel are 0.86° and 2° . Using Figure (13) and Schuler's Method (see Chapter IV), echo lengths indicate an in-slope of about 32° and an out-slope of 1° - 5° . This would indicate that on the in-slope in a direction perpendicular to the ship's track, there is a fairly large slope. Figure (16) shows the estimated ship's track over the Lone Rock/Quicks Hole area and verifies the fact that there is a steeper slope in a direction skewed to the ship's track.

210° 200° 190° 180° 170° 160° 150°
150° 160° 170° 180° 190° 200° 210°

BEAM PATTERNS
on
SEA BOTTOM
SINGLE LINE
&
MULTIPLY (V•T)

MULTIPLY
3dB Down

SINGLE LINE
3dB Down

FIGURE 12

330° 340° 350° 0 28 10° 20° 30°
30° 20° 10° 350° 340° 330°

140°
220°

130°
230°

120°
240°

110°
250°

100°
260°

90°
270°

80°
260°

70°
290°

60°
300°

50°
310°

40°
320°

QUICKS HOLE/LONE ROCK
UQN-1
TRANSMITTER & RECEIVER

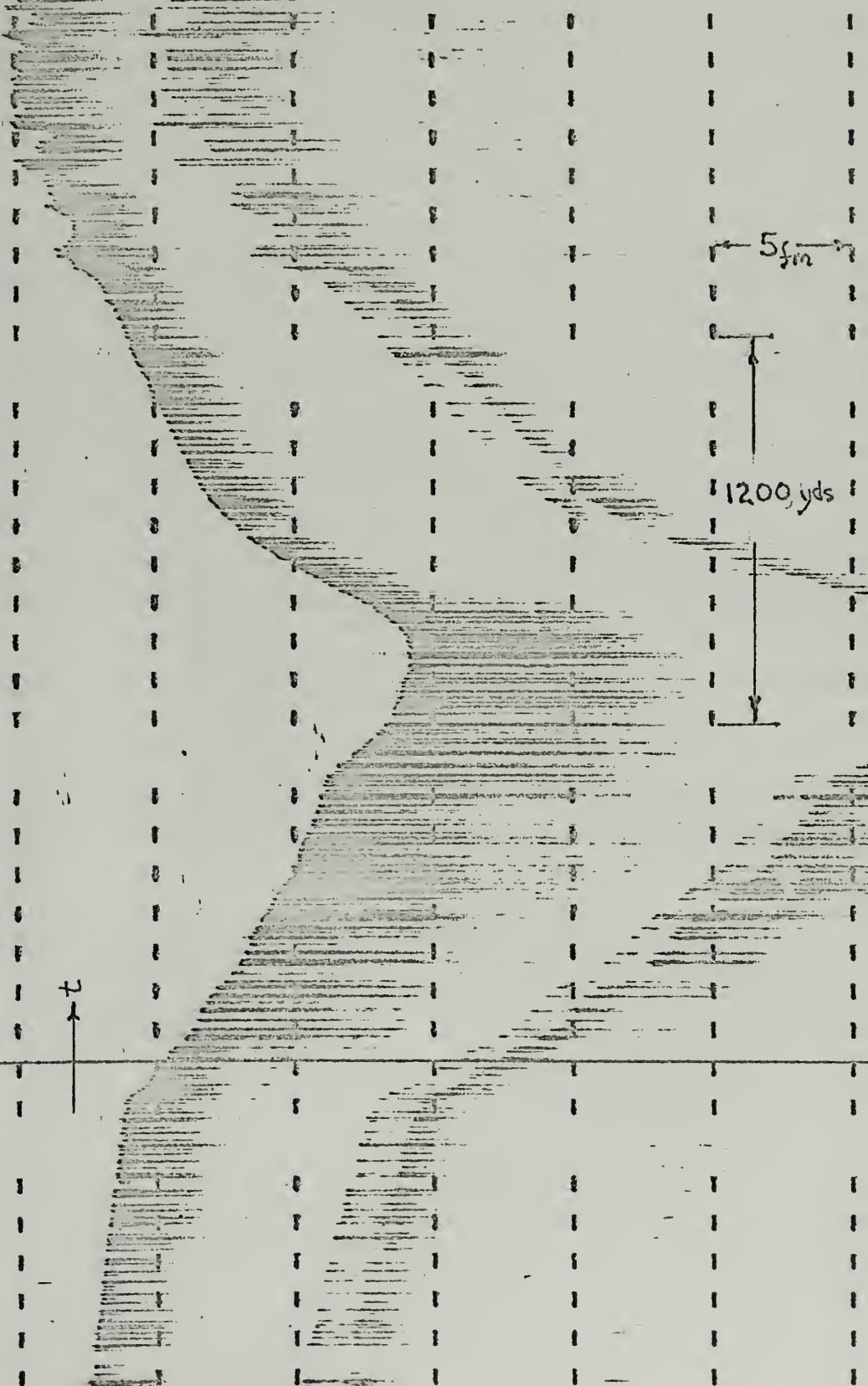


FIGURE (13)
29

QUICKS HOLE/LONE ROCK
V-PHONE (RECEIVER)
UQN (TRANSMITTER)

5fm

1200yds

QUICKS HOLE/LONE ROCK
T-PHONE (RECEIVER)
UQN (TRANSMITTER)

5 fm

1200 yds

C. & G. S. #263 LONE ROCK/QUICKS HOLE

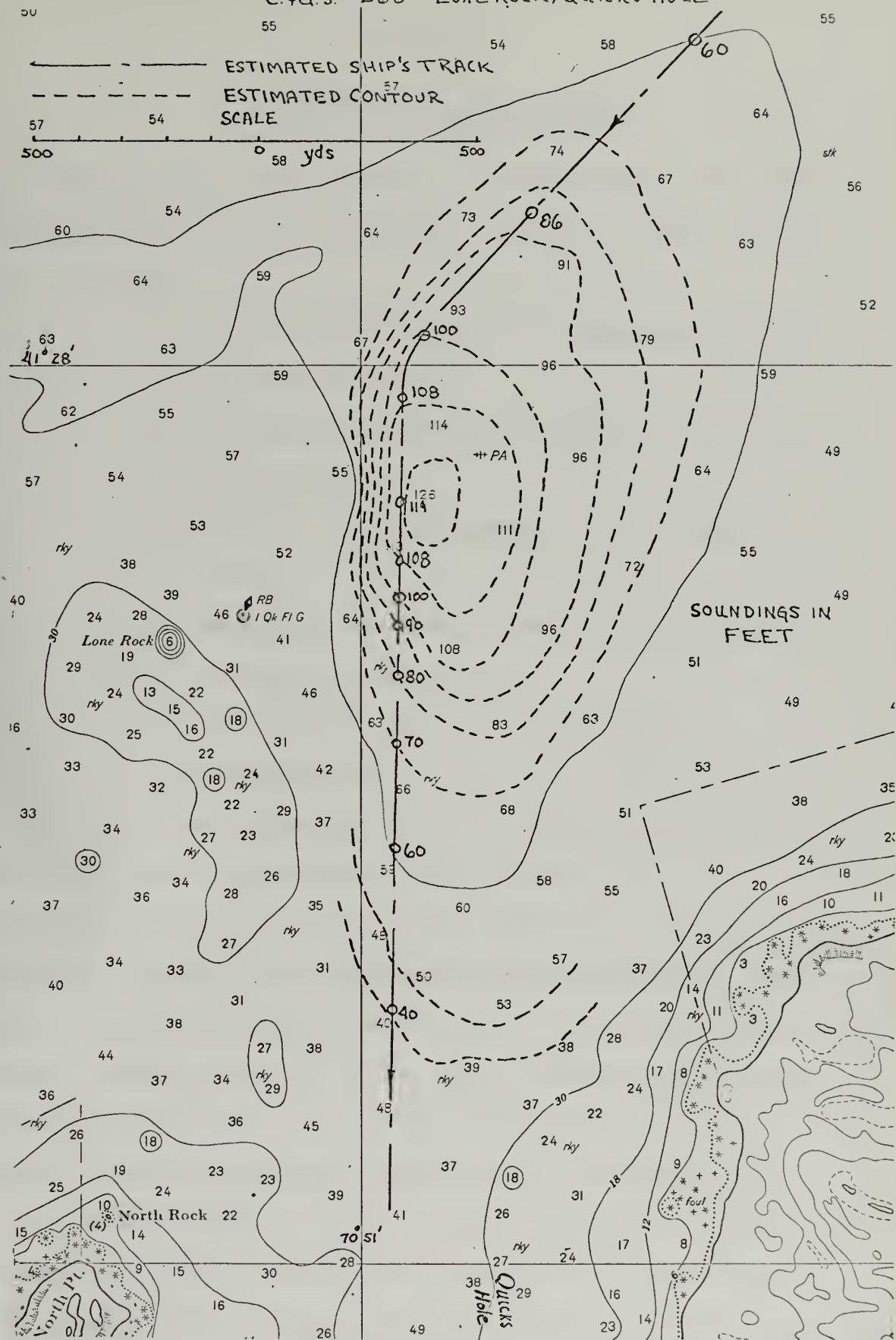


FIGURE 16
32

CHAPTER IV

INTERPRETATION OF ECHOGRAMS

The accurate determination of water depth and bottom topography is affected by several factors. These include the following:

- a) use of regionally generalized mean values of sound velocity
- b) directional patterns of acoustic radiators and receivers
- c) accuracy of measurement of echo travel time
- d) recording accuracy of returning echoes
- e) accuracy of navigation
- f) ship motions (speed, pitch, roll)
- g) reverberation

It has been shown by Gabler⁽⁶⁾ that between 1000 and 5000 meters water depth, the maximum error in sounding that occurs due to using mean sound velocity profiles is 5%. Timing and recording inaccuracies have been reduced to less than ± 2 meters. In an absolute sense, accurate navigation has much improved in the last few years through the use of electronic aids. In a relative sense, if a small area is to be examined, the use of buoys and/or bottom transponders limits navigation errors. The directional patterns of transmitter and receiver can provide the major source of bottom

profile errors. The basic reason stems from the fact that bottom surfaces are scanned by spherical caps of sound pulses. The bottom in turn acts as a collection of spherical radiators, and the fact that sonar transducers do not transmit or receive on a line means that equal transmitting times cannot be represented by a point but rather by a spherical cap. If the sea bottom is assumed to be a mirror, the ship will receive an echo from any part of the sea floor tangent to the spherical wave front as long as the reflection takes place within the half-angle of the transducer. Beyond that half-angle, the energy level of the sound ray is too low to activate the transducer on its return. This assumption is not valid over a steeply sloping (30°) bottom where the major echo will not return to the transducer and there will only be specular reflection. As a result, points lying on the same depth are shown with different times of transmission. In order to counteract the influence of such errors in recording the spherical angle of the radiating cone can be reduced. The tendency in wide cone transducers is an averaging of bottom topography; however, once the bottom has been recorded on a precision graphic recorder (PGR), the results must be interpreted. One general method of interpretation and more accurately determining bottom topography has been described by Schuler⁽¹⁹⁾ and is summarized as follows:

- a) Determine accurately the effective cone of the transducer
- b) Study the lines of the upper edge and the lower edge of the echo lengths with a view to the position of outstanding places and the echo extensions, because these are a direct measure of differences in the depth within the effective cone.
- c) Wherever a discontinuity occurs in the upper edge or wherever the lower edge is not parallel to the upper edge, differences exist between the profile drawn and the real profile.
- d) Depressions will already become evident half the length of the effective cone earlier before reaching the depression, which is caused by the increasing of the echo length. In the case of elevations, the aspect of the upper and lower borders is reversed.
- e) The lower boundary of the echo length is a better indication of the approximate shape of the profile.

Examples of Schuler's Method are described in Appendix (C).

Wide angle transducers have a composite type effect

on echogram recordings. A sloping bottom in general will not be accurately depicted on an echogram. Shalowitz and Krause⁽¹⁵⁾ have shown how slope correction procedures may be used, but these are often time consuming processes. In addition, they often do not work where bottom topography is irregular and complex. Krause, et.al.,⁽¹⁵⁾ have shown that for a sea floor of constant slope, the slope of the echogram was less than the sea floor and related by:

$$\sin\theta = \tan\xi$$

where $\tan\theta$ = true bottom slope

$\tan\xi$ = echo trace slope

This assumes that the beam width is great enough to obtain a perpendicular distance to the sea floor.

Narrowing the effective cone reduces the area of the bottom examined, and in this way much unwanted signal is removed. The narrower the beam, however, the more attention that must be made to array attitude. Since most array platforms have some response due to surface waves, it often becomes necessary to provide array stabilization via mechanical or electronic means. This in turn raises the cost and complexity of the system.

As suggested by Cohen⁽³⁾, bottom survey should be conducted with simultaneous operation of a narrow beam transducer and the standard wide beam transducer, with the respective profiles presented on separate recorders. Through the use of both records and Figure (17), the

bottom slope can be determined. This bottom slope computation depends on knowing the beam width of the narrow beam transducer and assumes that the slope/depth combination is such that a perpendicular distance to the bottom can be given by the wide angle transducer. It should be realized that if unstabilized, the cone axis may not be vertical.

BOTTOM SLOPE - DUAL RECORDING

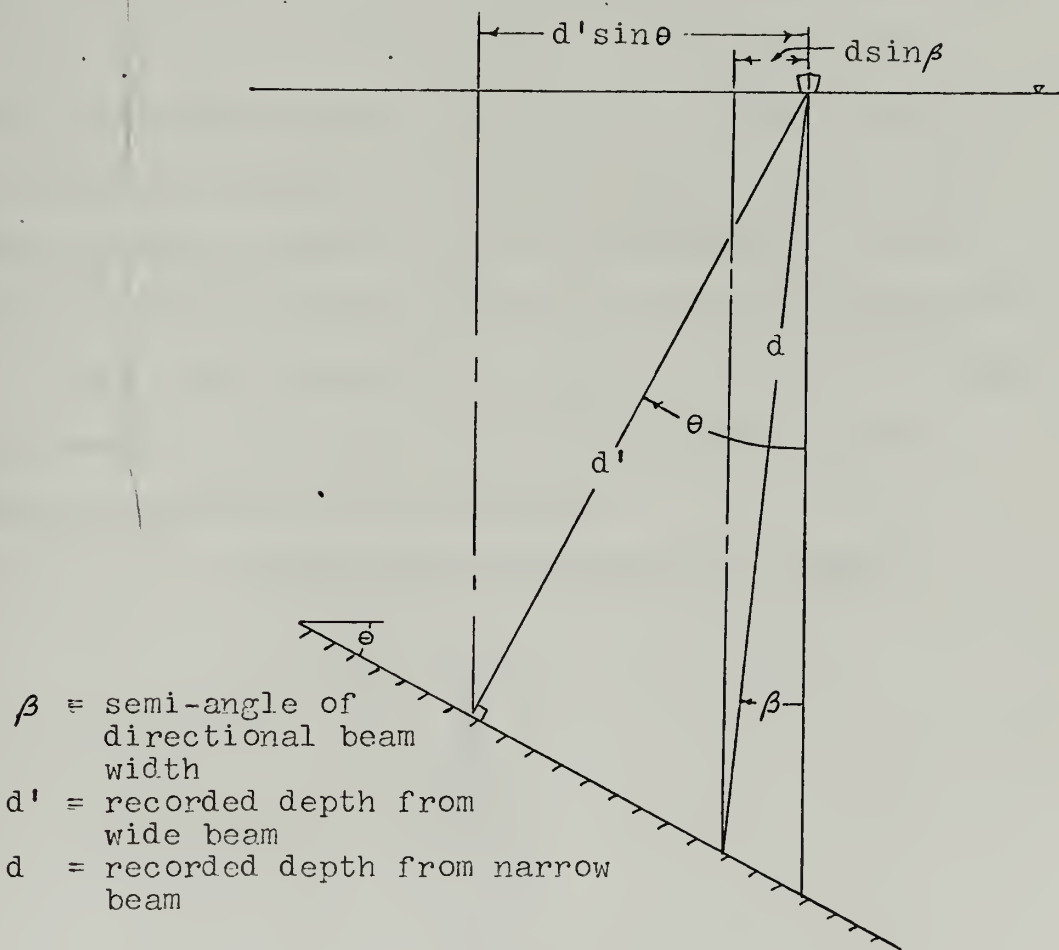


FIGURE 17

From Figure (17):

$$\tan \theta = \frac{d \cos \beta - d' \cos \theta}{d' \sin \theta - d \sin \beta}$$

and $\frac{d'}{d} = \cos(\theta - \beta)$

Simultaneous recording can be used as a good check of the ship's track. If both records show the same depth over an object such as a seamount, this indicates that the ship passed directly over the mount. A depth difference is an indication of the horizontal distance from the seamount.

Ship motion (pitch and roll) will often cause amplitude fluctuations in the incoming signal that can be seen best on an oscilloscope. In the case of a stabilized beam and no ship motions, fluctuations may be caused by contours on the sea bottom. These fluctuations can be manipulated using statistical theory and some idea of bottom roughness can be determined.⁽⁷⁾

Ship speed can have an effect on accuracy of depth measurements. If a wide angle echo sounder is used, several relations can be obtained.

DEPTH CORRECTION FOR SHIP'S SPEED

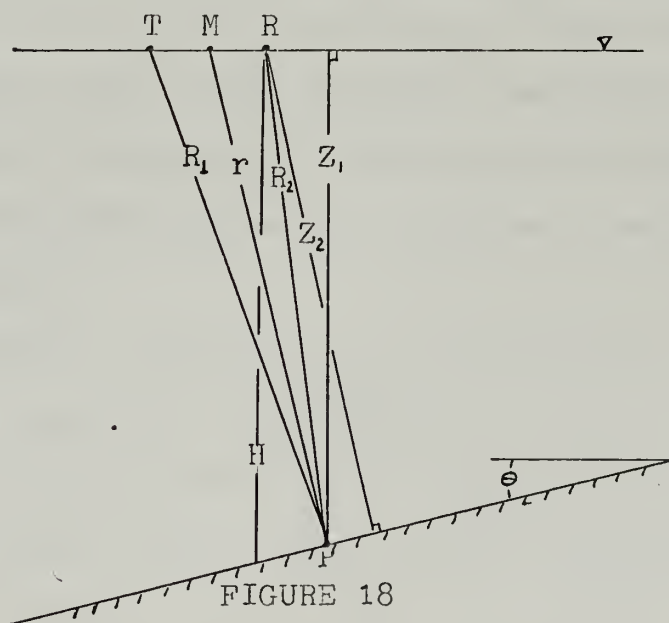


FIGURE 18

The recorded depth is equal to $\frac{R_1 + R_2}{2}$, but the actual depth at the time of recording, ship at R, is "H". Then the depth error, " Δr ", is equal to $\left[\frac{R_1 + R_2}{2} - H \right]$. However, this function will have bottom slope effects in it as described earlier. In order to have only "ship forward motion" effects, examine $\left[\frac{R_1 + R_2}{2} - z_2 \right]$. This will give the difference between recorded depth and the depth "seen" by the wide angle echo sounder at the receiving position R.

Let $\Delta S = \left[\frac{R_1 + R_2}{2} - z_2 \right]$, and by geometry

$$\Delta S = \frac{z_1}{\cos \theta} \left[\frac{\sqrt{1 - \left(\frac{v_s}{v_a}\right)^2 \cos^2 \theta}}{1 - \left(\frac{v_s}{v_a}\right)^2} - \frac{\sqrt{1 - \left(\frac{v_s}{v_a}\right)^2 \cos^2 \theta}}{\sqrt{1 - \left(\frac{v_s}{v_a}\right)^2 \cos^2 \theta} + \frac{v_s}{v_a} \sin \theta} \right]$$

The results of a sample calculation is shown for:

$z_1 = 15,000$ feet, $v_s = 12$ knots, $v_a = 4800$ feet/sec.

$\theta = 30^\circ$: $\Delta s = 36$ feet

Reverberation is a general name used to describe signals reflected by objects in the sea other than the target. In the case of echo-sounding, these objects include bubbles, fish, kelp, suspended particles, and inhomogeneities in the water. These unwanted signals may return at the same time as the bottom echo masking the desired signal.

Volume reverberation is defined as:

$$R_V = .10 \log \left[\eta_v V \frac{I_{BS}}{I_i} \right], \text{ dB re } r_0$$

where: V is active volume proportional to sound source cone angles, range squared, and pulse length

η_v is number of scatterers in the volume

I_{BS} is backscattered intensity

I_i is incident intensity

$$\text{Now: } I_{BS} \triangleq \frac{I_i \sigma_v}{4\pi r_o^2}$$

where σ_v is defined as scattering cross section

r_o is reference range

$$\text{Since: } V = \frac{ab r^2 c\tau}{2}$$

where a, b are cone angles

$c\tau$ is pulse length

$$\text{Then: } VR_S = 10 \log \frac{\eta_v \sigma_v}{4\pi} + 10 \log \frac{ab r^2 c\tau}{2 r_o^2}, \text{ dB re } r_o$$

In a similar manner surface reverberation is:

$$R_S = 10 \log \frac{\eta_A \sigma_A A}{2\pi r_o^2}, \text{ dB re } r_o$$

where: η_A = scatterers per unit area

σ_A = scattering cross section

A = illuminated area

Reverberation can be reduced by having small cone angles, short pulse length, and short range. The environmental factor ($\eta\sigma$) is a function of frequency, depth (for $\eta_v \sigma_v$) and bottom type (for $\eta_A \sigma_A$).

CHAPTER V

EFFECTS OF SOUND VELOCITY PROFILE AND REFRACTION

Straight line approximations and mean sound velocities are used in both Chapter IV and Appendix (C), and they introduce inaccuracies in the values of water depth and echo length. The inaccuracies introduced by the use of mean sound velocities are discussed by Gabler⁽⁶⁾ and Maul⁽¹⁶⁾. What is examined here are two specific examples using an assumed velocity profile (Figure 19), water depth, and two projector cone angles.

ASSUMED SOUND VELOCITY PROFILE

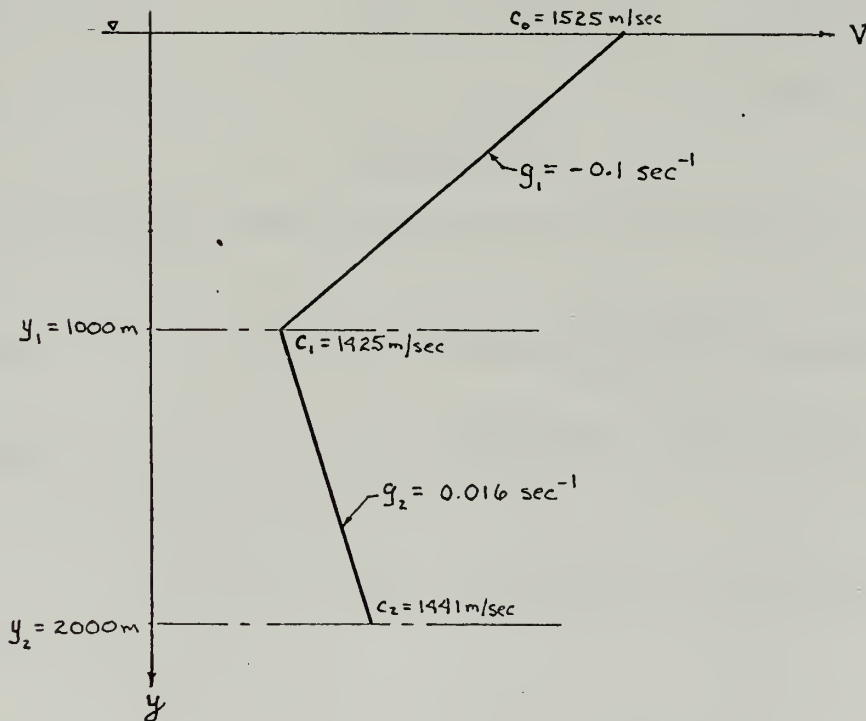


FIGURE 19

Three models are considered:

- a) Constant "machine" sound velocity
- b) Mean sound velocity (no refraction)
- c) Velocity profile and refraction

The specific values to be computed and compared are time differences as described in Figure (20).

TIME/SOUND PATH MODELS

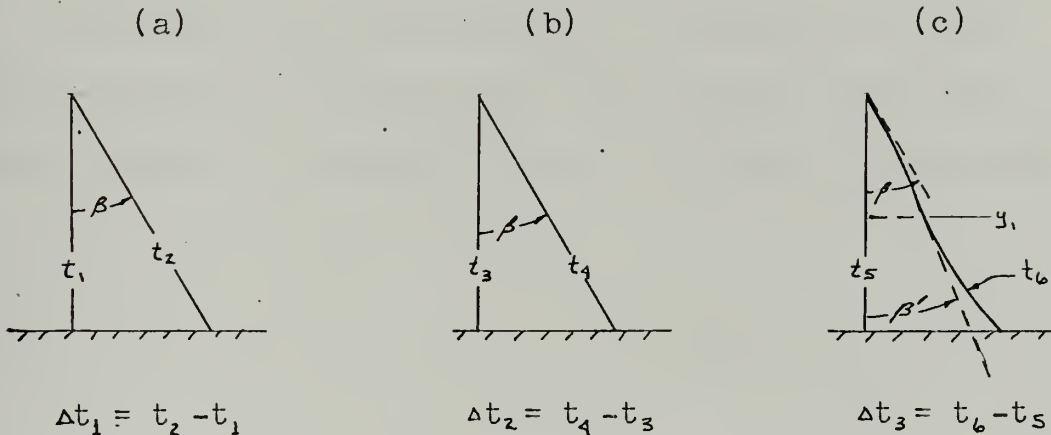


FIGURE 20

The formulas used for computing the various times are:

Model (a) $t_{1,2} = \frac{\text{Distance}}{\text{Constant sound velocity (1465 m/sec)}}$

Model (b) $t_{3,4} = \frac{\text{Dist. } |_{0-1000}}{\bar{c}_{0-1000}} + \frac{\text{Dist. } |_{1000-2000}}{\bar{c}_{1000-2000}}$

$$t_5 = \frac{1}{g_1} \ln \left[\frac{g_1 y_1 + c_0}{c_0} \right] + \frac{1}{g_2} \ln \left[\frac{g_2 (y_2 - y_1) + c_1}{c_1} \right]$$

Model (c)

$$t_6 = \frac{1}{g_1} \ln \left\{ \frac{\tan \left[\frac{\sin^{-1} \left(\frac{c_1}{c_0} \sin \beta \right)}{2} \right]}{\tan(\beta/2)} \right\} + \frac{1}{g_2} \ln \left\{ \frac{\tan \left[\frac{\sin^{-1} \left(\frac{c_2}{c_1} \sin \beta' \right)}{2} \right]}{\tan \left[\frac{\sin^{-1} \left(\frac{c_1}{c_0} \sin \beta \right)}{2} \right]} \right\}$$

The results of these computations are shown in Table (2).

ECHO LENGTH TIMING ERRORS

	Echo Length (sec)			Echo Length Errors (sec)	
	Δt_1	Δt_2	Δt_3	$\Delta t_3 - \Delta t_1$	$\Delta t_3 - \Delta t_2$
$\beta = 30^\circ$	0.212	0.213	0.251	0.039	0.038
$\beta = 10^\circ$	0.2045	0.02065	0.043	0.02255	0.02235

TABLE 2

If Model (c) is considered to represent a close approximation to reality, then echo length errors can significantly be reduced by using the smaller cone angle.

CHAPTER VI

CONCLUSIONS

There is good correlation between the theoretical and experimental data on the beam patterns of a shaded line hydrophone. Both show a major lobe beam width of 10° at dB down. The effects of baffling, tube diameter and tube out-of-roundness probably caused much of the differences between the beam patterns.

It should be recognized that a large portion of the ocean bottom, in particular the canyons of the Continental Shelf, are not a smooth constant slope, but rather the area covered by the hydrophone will be very complex. This area will be fairly large; over 10^6 sq. ft. for a 12° cone angle at 6000 ft., and about 3×10^4 sq. ft. for a 6° cone angle at 6000 ft. The advantage of narrowing the cone angle is that the area covered will be smaller and thus give higher resolution.

It should also be recognized that the ideal single conical beam pattern in reality has side lobes, and they may effectively widen the beam pattern over a sloping bottom. As an example, for a side lobe 14 dB down at $12\frac{1}{2}^{\circ}$ from the main beam, the side lobe will begin to interfere on a sloping bottom of 74.2° at a depth of 6000 ft. Reducing the depth to 3000 ft. will reduce the limiting slope to 53.6° . For a side lobe only 4 dB down at $12\frac{1}{2}^{\circ}$ from the main beam the side lobe

will begin to interfere on a sloping bottom of 40° at a depth of 6000 ft. Over the range of depth and side lobe intensity, their interference will be minimum.

No new information, over what is readily obtainable on C&GD Chart #263, was obtained from the crossed hydrophone array during the single pass over the Lone Rock/Quicks Hole area; however, practical application of the use of echo length was verified for this shallow water experiment.

By multiplying the outputs of the two line hydrophones a narrow "pencil beam" was obtained. It approximated a cone with an aperture angle of about 10° at 10 dB down. The signal processor is considered only adequate. More careful filtering, less internal noise, and more amplification should be done if further work is to be done in this area. An alternate solution would be the use of a variable phase shifter in the outputs of the two hydrophones and then add the two signals. This process is similar to that which is often used in the fabrication of circular arrays and this solution would be preferred for low signal to noise ratios. Another solution would be the use of a transducer that already exhibits a narrow, symmetrical cone angle such as EDO Model 202 as described in Appendix (F).

The engineering design and mounting of the crossed array needs modification if continued use is desired since flow noise was excessive. It is suggested that

although flow noise is not excessive at speeds of 3 knots or less, an acoustically transparent cover be provided for the crossed array to improve its hydrodynamic characteristics. Air bubbles are apparently being carried along the bottom of the hull causing partial blockage of the acoustic signal. Mounting of the array in a recessed well or outside this bubble layer should be considered.

Narrowing the cone angle will have the additional benefit of reducing refraction errors in the measurement of echo length.

The use of a simplified sound velocity profile would enhance the capabilities of the depth sounder, give a more accurate value of depth and echo length, all leading towards a more accurate value of bottom slope.

CHAPTER VII

RECOMMENDATIONS

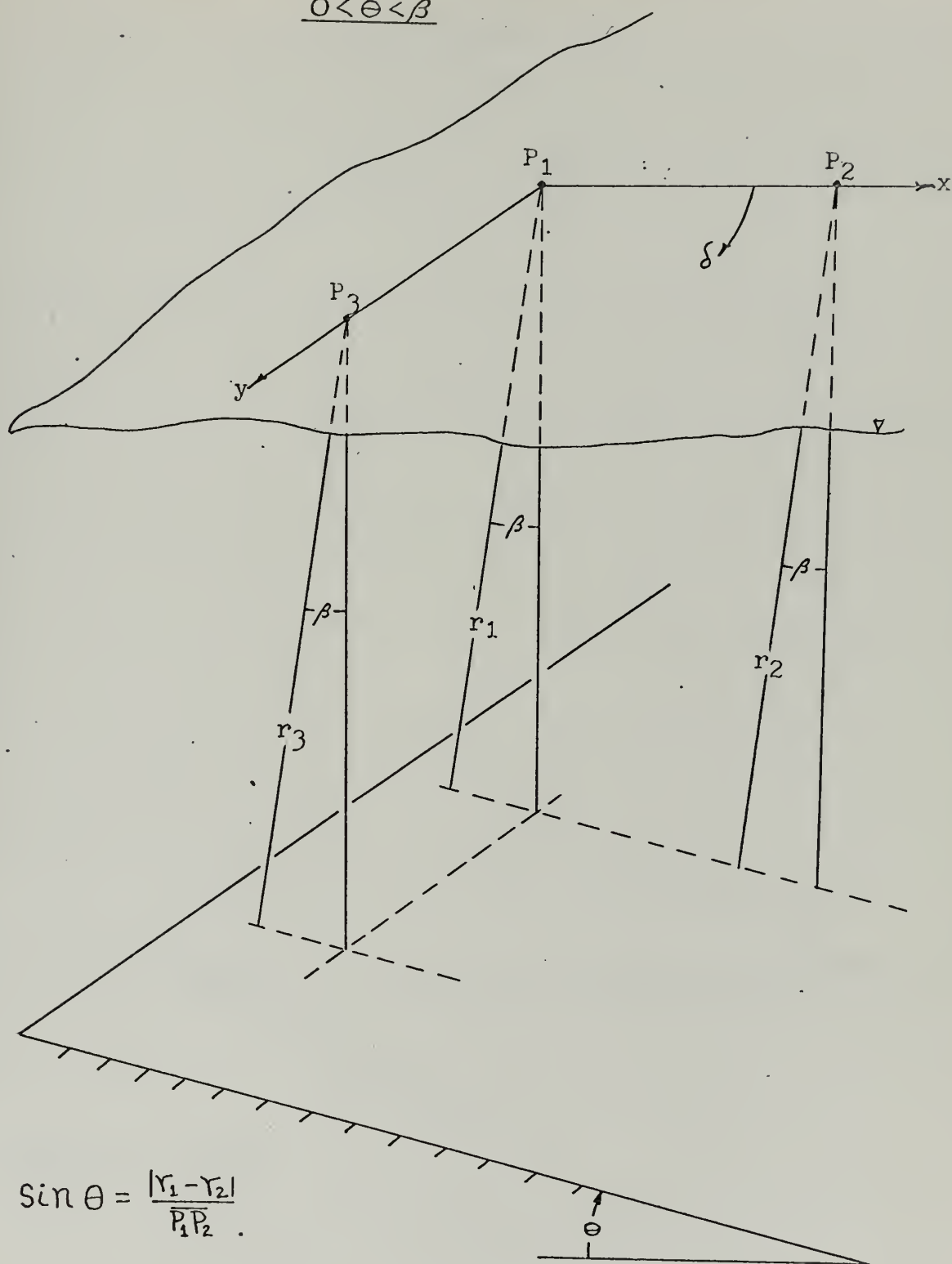
Upon completion of this fairly narrow investigation, it appears that a possible area for further investigation might be in the area of simple computerization to reduce the data gathered in an automatic manner in real time. This is not to discount the work done in computerizing data reduction done by Harris ASW Division of General Instrument Corporation and Ross Laboratories, Inc., for the National Ocean Survey; however, it would seem that a fairly cheap and simple computer could be designed to provide bottom slope and actual water depth using a hydrophone with a medium aperture angle. What is suggested is a computing system that would solve the simple geometry described in Appendix (C), where with some estimate of bottom slope, a mode could be selected and the output would be water depth, time average bottom slope, and instantaneous bottom slope. The instantaneous slope can be found by automating the procedure described in Appendix (C), with the first return travel time and echo length as inputs.

The time average slope would be that derived from knowledge of first return times and ship's velocity. Figures (21) and (22) describe how time average slope can be computed. Note that if the ship is traveling perpendicular to the bottom slope that $r_1 = r_2$ and zero slope will be indicated. By comparing time average to

instantaneous slope the skew angle of the slope can be found. Care should be taken to realize the limitations of the simple geometric assumptions made in this illustration. The actual bottom topography will probably be complex and this model will no longer hold. What such a system would offer would be a ready source of three more bits of data that the oceanographer could use along with the normal echogram to make a more accurate estimate of the bottom topography.

BOTTOM SLOPE - INSTANTANEOUS/TIME AVERAGE

$$0 < \theta < \beta$$



$$\sin \theta = \frac{|r_1 - r_2|}{P_1 P_2}$$

FIGURE 21

BOTTOM SLOPE - INSTANTANEOUS/TIME AVERAGE

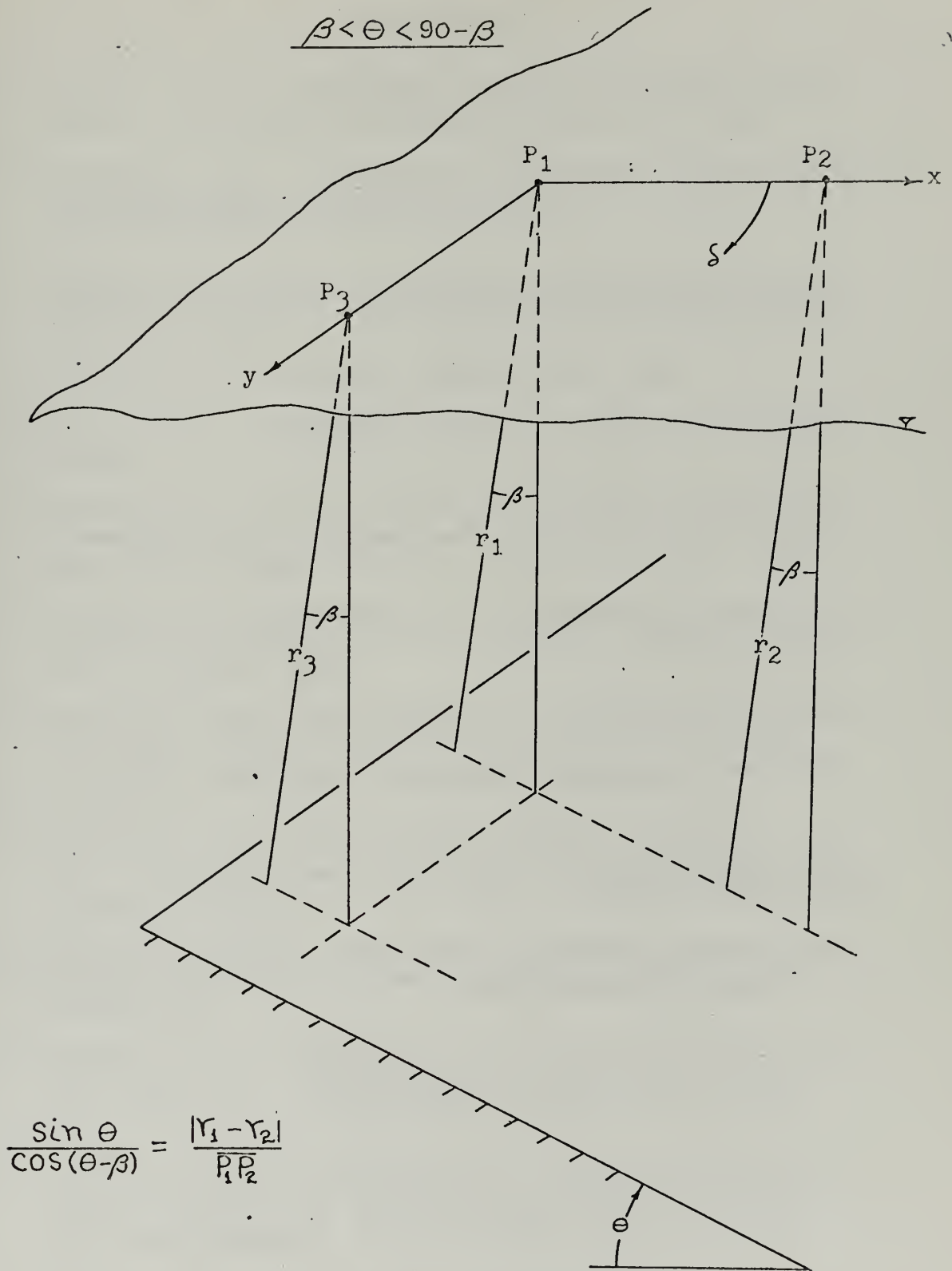


FIGURE 22

BIBLIOGRAPHY

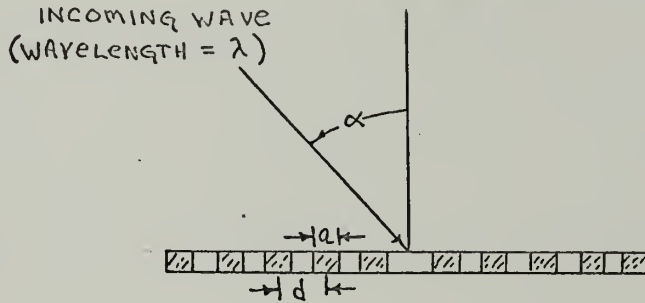
1. Albers, V.O., UNDERWATER ACOUSTICS HANDBOOK, Penn. State Univ. Press, University Park, Pa., 1960.
2. Carstens, R.H., "Problems in Fathogram Interpretation", International Hydrographic Review, Vol. XXXI, No. 2, November 1954, p. 115.
3. Cohen, P.M., "Directional Echo Sounding on Hydrographic Surveys", International Hydrographic Review, Vol. 36, 1959.
4. Dietrich, G., GENERAL OCEANOGRAPHY, 1963.
5. Fay, H.J.W., SUBMARINE SIGNAL LOG, Raytheon Company, 1963.
6. Gabler, H., "On the Limits of Accuracy in the Echo Soundings of Ocean Regions", Trans-107, USN Oceanographic Office, 1962.
7. Gazey, B.K., "Sea-bed Echo Amplitude Fluctuations Arising from Ship Motion", J. Brit. I.R.E., Vol. 26, No. 2, August 1963.
8. Haslett, R.W.G. and Honnor, D., "Simultaneous use of Sideways Looking Sonar, Strata Recorder and Echo Sounder", Radio and Electrical Engineer, June 1967, p. 361.
9. Hickley, R.J., "Some Recent Systems Development by U.S. Coast and Geodetic Survey", International Hydrographic Review, Vol. XLII, No. 1, January 1965, p. 41.
10. Huestis, T.H.W., "The Coast & Geodetic Survey gets Narrow Beam Echo Sounder", Undersea Technology, June 1964.
11. Hurley, R.J., "Bathymetric Data from the Search for USS Thresher", International Hydrographic Review, Vol. XLI, No. 2, July 1964, p. 43.
12. Knott, S.T. and Hersey, J.B., "Interpretation of high-resolution echo-sounding techniques and their use in bathymetry, marine geophysics, and biology", Deep Sea Research, Vol. 4, 1965, p. 36.
13. Knott, S.T., "Use of the Precision Graphic Recorder (PCR) in Oceanography", MARINE SCIENCES INSTRUMENTATION, Vol. 1, 1962.

14. Konrad, W.L., "Final report-Study of Finite Amplitude Effects in Underwater Sound Propagation", Raytheon Company, Contract No. N00140-69-C-0173.
15. Krause, D.C., "Interpretation of Echo Sounding Profiles", International Hydrographic Review, Vol. 39, No. 1, January 1962.
16. Maul, G.A., "Precision Echo-Sounding in Deep Water", International Hydrographic Review, Vol. XLVII, No. 2, July 1970.
17. OCEAN ENGINEERING, A preliminary report submitted to the Chairman of the Interagency Committee of Oceanography, Vol. 3, March 1966.
18. Schuler, D.I., "Echogram Profiles and how they can be established", International Hydrographic Review, Vol. XXXIV, No. 2, November 1957, p. 41.
19. Schuler, E.F., "On the Accuracy of Configuration of Sea Bottom Profiles with HF Echo Sounders", International Hydrographic Review, Vol. 29, 1952.
20. Tucker D.G. and Gazey, B.K., APPLIED UNDERWATER ACOUSTICS, 1966.
21. Tucker, D.G., "Directional Echo Sounding ", International Hydrographic Review, Vol. XXXVII, No. 2, July 1960, p. 43.
22. Tucker, D.G., "Multiplicative Arrays in Radio-Astronomy and Sonar Systems", J. Brit. I.R.E., Vol. 25, No. 2, February 1963.
23. Urick, R.J., PRINCIPLES OF UNDERWATER SOUND FOR ENGINEERS, 1967.

APPENDIX (A)

ANALYTICAL DEVELOPMENT FOR COMPUTER PROGRAM

The beam pattern of a linear array of elements of finite length can be considered in two parts.



The two parts consist of the direction pattern of an individual element, and the direction pattern of a corresponding linear point array. Assume that the incoming signal is a plane wave, that the wave received at the center is $\cos \omega t$ and normalized to unity, and that the array is symmetrical about the centerline.

The output voltage of all the elements in series will be the product of the individual element pattern with the sum of the point voltages.

$$\text{For the single element, } u(\alpha) = \int_{-a/2}^{a/2} \frac{1}{a} \cos \left[\frac{2\pi r}{\lambda} \sin \alpha \right] dr$$

This assumes that the taper function of the element is constant over its length and equals $\frac{1}{a}$. Then $u(\alpha) = \frac{\sin \left[\frac{\pi a}{\lambda} \sin \alpha \right]}{\frac{\pi a}{\lambda} \sin \alpha}$

The voltage output of ten point sources will be:

$$w(\alpha) = \sum_{k=1}^{10} R_k \cos \left[\frac{2k-1}{2} \cdot \frac{2\pi d}{\lambda} \sin \alpha \right]$$

where R_k are the shading factors of the individual elements.

In the JT hydrophone the R_k are symmetrical about the centerline and are equal to 9.2, 14.0, 25.0, 38.8, 50.0; therefore: $w(\alpha) = 2 \sum_{k=1}^5 R_k \cos \left[\frac{2k-1}{2} \cdot \frac{2\pi d}{\lambda} \sin \alpha \right]$

The overall beam pattern in dB, normalized to unity at

$$\alpha = 0 \text{ is : } V(\alpha) = 20 \log. \left[\frac{u(\alpha)w(\alpha)}{2 \sum_{k=1}^5 R_k} \right]$$

APPENDIX (B)

COMPUTER PROGRAM

C THIS PROGRAM WILL COMPUTE BEAM PATTERNS FOR LINE ARRAYS
C OF ELEMENTS OF FINITE LENGTH WHERE L=WAVELENGTH, D=
C ELEMENT TO ELEMENT SEPARATION, A=ELEMENT LENGTH, AA=
C ELEMENT DIRECTION PATTERN, BB=PATTERN IN DB, R=ELEMENT
C SHADING FACTORS, BETA=SKUEW ANGLE, YTEMP=ARRAY FACTOR.
C THIS COMPUTATION IS DONE FOR VARIOUS SKEW ANGLES. THE
C GIVEN DATA IS FOR A FIVE FOOT LINE HYDROPHONE AT 12KHZ
C WITH LINEAR TAPER ASSUMED FOR EACH ELEMENT.

REAL L

DIMENSION R(10),L(5),AA(90),BB(90)

D=5.85

A=5.75

READ(5,100) (L(I),I=1,5)

100 FORMAT(5F6.2)

READ(5,101) (R(I),I=1,10)

101 FORMAT(10F6.2)

RSUM=0.0

DO 9 I=1,10

9 RSUM=RSUM+R(I)

N=1

WRITE(6,201)

201 FORMAT(19X,'SHADING FACTORS',34X,'RSUM',7X,'SEPARATION
1 WAVELENGTH ELEMENT LENGTH')

WRITE(6,200) (R(I),I=1,10),RSUM,D,L(N),A

200 FORMAT(2X,10F6.2,4F12.3)

BETA=0.0

ZETA=0.0

3 WRITE(6,300)

300 FORMAT(2X,'SKEW ANGLE ROTATION ANGLE ELEM DIR PAT
1 PATTERN(DB)')

WRITE(6,400) BETA

400 FORMAT(5X,F4.1)

DO 12 I=1,90

WTEMP=I*COS(ZETA)/57.3

UTEMP=6.2832*D*SIN(WTEMP)/L(N)

2 YTEMP=2*(R(1)*COS(4.5*UTEMP)+R(2)*COS(3.5*UTEMP)+
1R(3)*COS(2.5*UTEMP)+R(4)*COS(1.5*UTEMP)+R(5)*COS(0.5
2*UTEMP))

AA(I)=SIN(0.5*A*UTEMP/D)/(0.5*A*UTEMP/D)

BB(I)=10ALOG10((AA(I)*YTEMP/RSUM)**2)

WRITE(6,401) I,AA(I),BB(I)

401 FORMAT(19X,I2,8X,2F12.6)

12 CONTINUE

BETA=BETA+5.0

ZETA=BETA/57.3

IF(BETA.EQ.95) GO TO 20

GO TO 3

20 STOP

END

APPENDIX (C)

EXAMPLES OF SCHULER'S METHOD

The following examples will describe the use of echo length to determine the actual bottom configuration. First the aperture angle of the echo sounder should be known or computed, and from this an expected echo length on a flat bottom can be found.

CASE I

ECHO LENGTH - FLAT BOTTOM

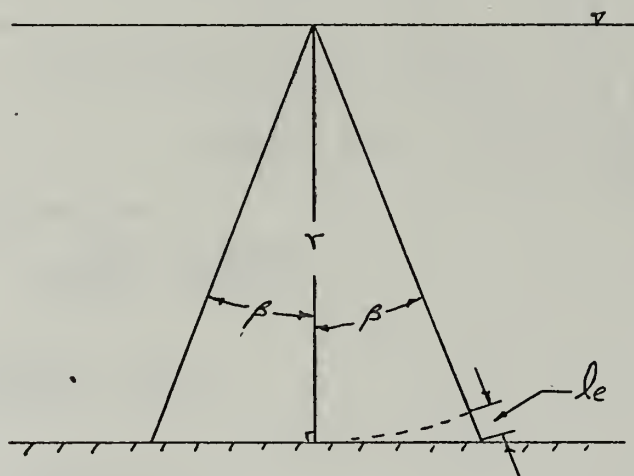


FIGURE (23)

With an aperture angle of 2β ,

$$\ell_e = r \left[\frac{1 - \cos \beta}{\cos \beta} \right]$$

- EXPECTED ECHO LENGTH

where r = recorded depth.

CASE II

Now consider that one half the transducer's effective cone includes a slope.

ECHO LENGTH - FLAT/SLOPE TRANSITION

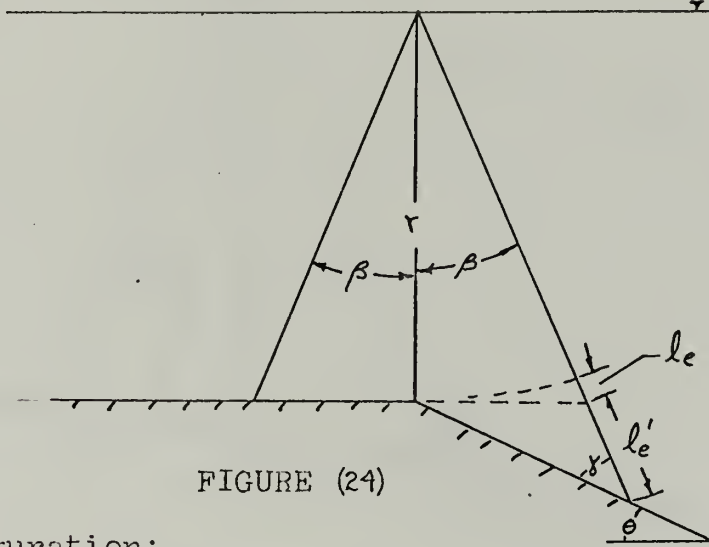


FIGURE (24)

For this configuration:

$$\frac{l_e'}{\sin \theta} = \frac{r \tan \beta}{\sin \gamma}$$

Or:

$$l_e' = \frac{\sin \theta}{\sin \gamma} r \tan \beta$$

But: $\sin \gamma = \cos(\beta + \theta)$

Then: $l_e' = \frac{\sin \theta}{\cos(\beta + \theta)} r \tan \beta$

And: $l_e'' = l_e + l_e' = r \left[\frac{1 - \cos \beta}{\cos \beta} + \frac{\sin \theta \tan \beta}{\cos(\beta + \theta)} \right]$ - TOTAL ECHO LENGTH

Now consider the complete cone covering the slope.

CASE III: $0 < \theta < \beta$

ECHO LENGTH - SHALLOW SLOPE

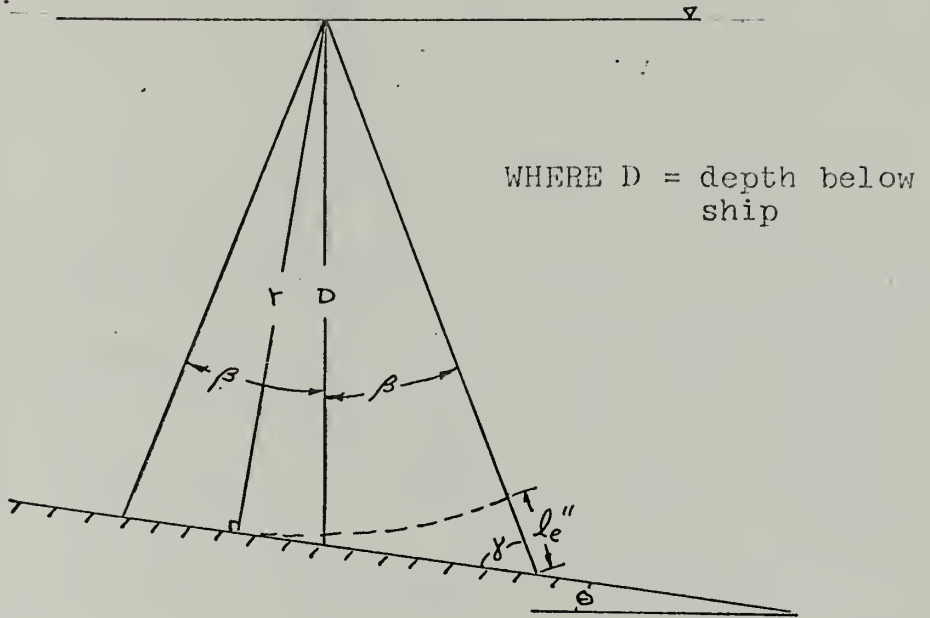


FIGURE (25)

For this configuration:

$$l_e'' = r \left[\frac{1}{\sin \gamma} - 1 \right]$$

$$l_e'' = r \left[\frac{1 - \cos(\beta + \theta)}{\cos(\beta + \theta)} \right]$$

And: $D = \frac{r}{\cos \theta}$

CASE IV:

ECHO LENGTH - STEEP SLOPE

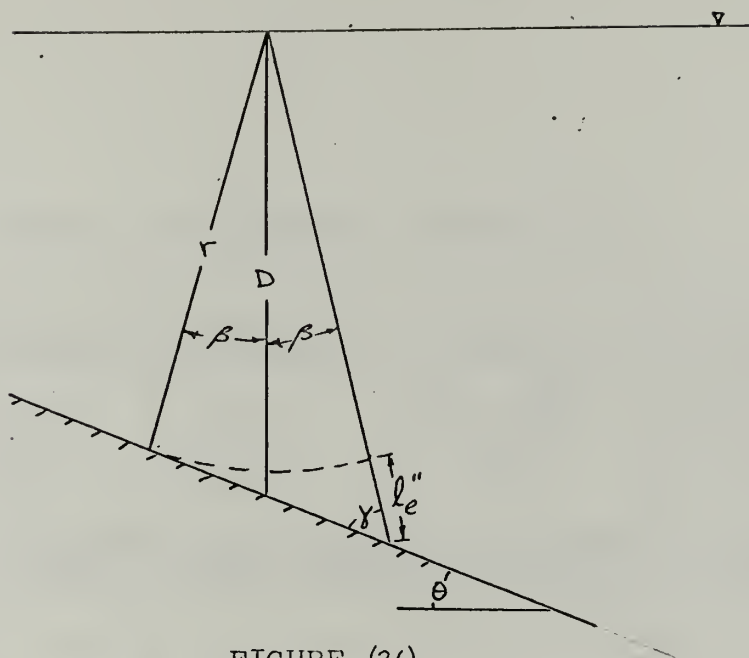


FIGURE (26)

For this configuration:

$$\frac{2(r \cos \beta) \tan \beta}{\sin \gamma} = \frac{l_e''}{\sin \theta}$$

Or:

$$l_e'' = \frac{\sin \theta}{\cos(\beta + \theta)} \cdot 2r \sin \beta$$

And:

$$D = \frac{\cos(\theta - \beta)}{\cos \theta} \cdot r$$

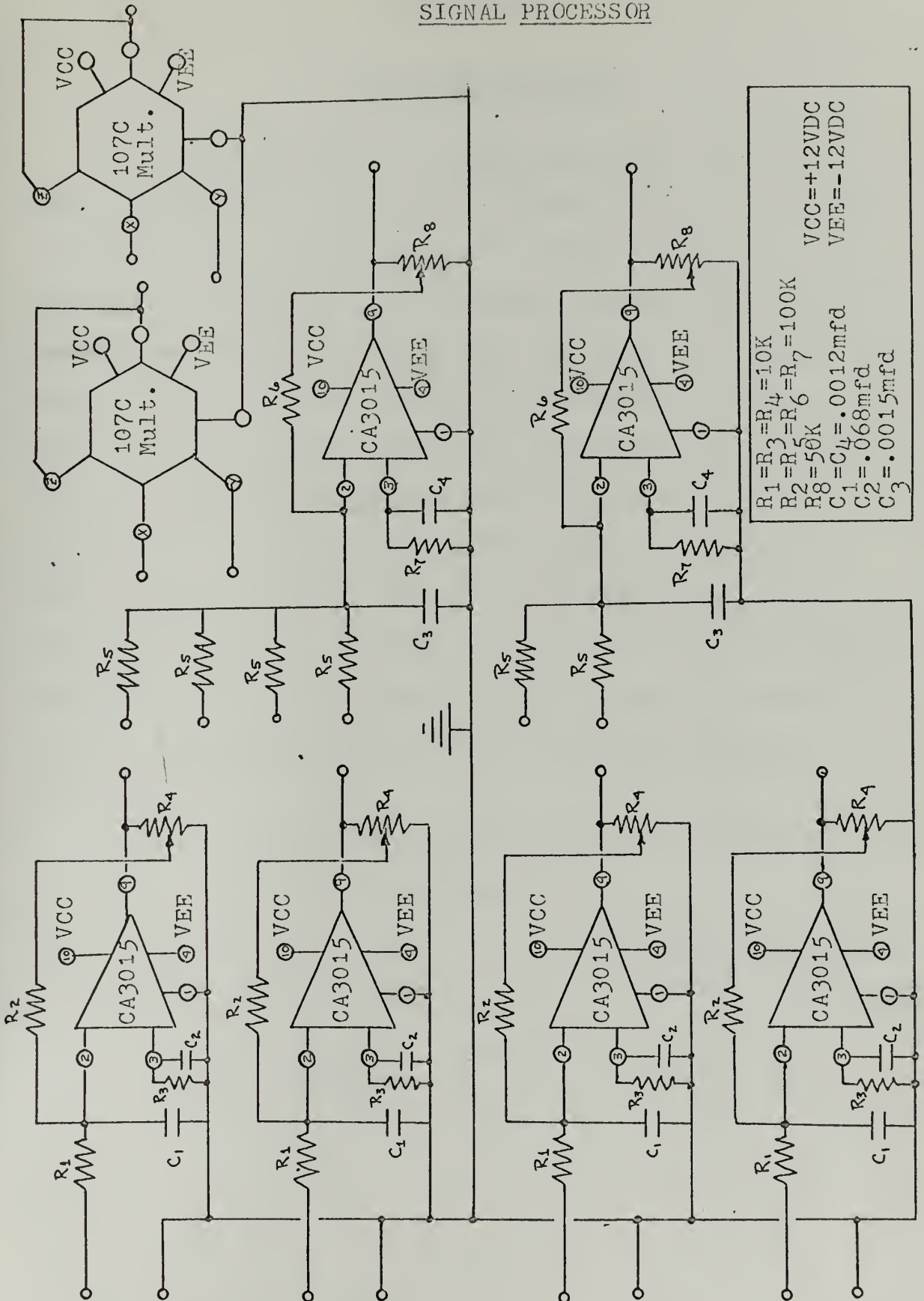
To summarize, the Table (3) is presented to give relations between actual depth, echo length, recorded depth and bottom slope. These calculations include only very simple bottom topography with no attempt made to account for the effects of absorption, reflection factor, amplification on echo length. Somewhat more complex bottom topography is treated by Krause.

DEPTH - ECHO LENGTH - BOTTOM SLOPE

	CASE I	CASE II	CASE III	CASE IV
ACTUAL DEPTH (D)	$D = r$	$D = r$	$D = \frac{r}{\cos \theta}$	$D = r \left[\frac{\cos(\theta - \beta)}{\cos \theta} \right]$
ECHO LENGTH (l_e'')	$l_e'' = r \left[\frac{1 - \cos \beta}{\cos \beta} \right]$	$l_e'' = r \left[\frac{1 - \cos \beta}{\cos \beta} + \frac{\sin \theta \tan \beta}{\cos(\beta + \theta)} \right]$	$l_e'' = r \left[\frac{1 - \cos(\beta + \theta)}{\cos(\beta + \theta)} \right]$	$l_e'' = \frac{2r \sin \beta \sin \theta}{\cos(\beta + \theta)}$
BOTTOM SLOPE $f(\theta)$	$\theta = 0$	$\tan \theta = \frac{(l_e'' + r) \cos \beta - r}{(l_e'' + r) \sin \beta}$	$\cos(\beta + \theta) = \frac{r}{r + l_e''}$	$\tan \theta = \cot \beta \left[\frac{l_e''}{2r + l_e''} \right]$
BOTTOM SLOPE (β SMALL)			$\theta = \left[\frac{l_e''}{2r} \right]^{1/2}$	$\tan \theta = \frac{l_e''}{2r \beta}$

TABLE (3)

SIGNAL PROCESSOR



APPENDIX (E)

JT HYDROPHONE DATA

The JT hydrophone is a magnetostrictive tube type unit divided into two identical halves mounted in-line on a central axis. Each half has an effective length of $2\frac{1}{2}$ feet, and consists of five sections. Each section is composed of a split nickel tube provided with a permanent magnet across its open ends to form a closed cylinder. Each section is toroidally wound with varying amounts of wire with nominal resistance values of 50Ω , 38Ω , 25Ω , 13.8Ω , and 9Ω . This shading will reduce side lobes and narrow the main beam. Section dimensions are $1\frac{15}{64}$ " x $5\frac{11}{16}$ " with a slot $5/16$ " wide along its length for the permanent magnet. A "pc" rubber boot is used to seal and protect mechanical components and provides an outer casing for the hydrophone.

The following additional data was collected during testing at the Boston Naval Shipyard:

	V Phone	H Phone
Receiving Response (dB/ μ bar/volt)	-90.5	-88.5
Impedance (Ohms/degrees @ 12 kHz @ 10 volts)	330/57	520/40

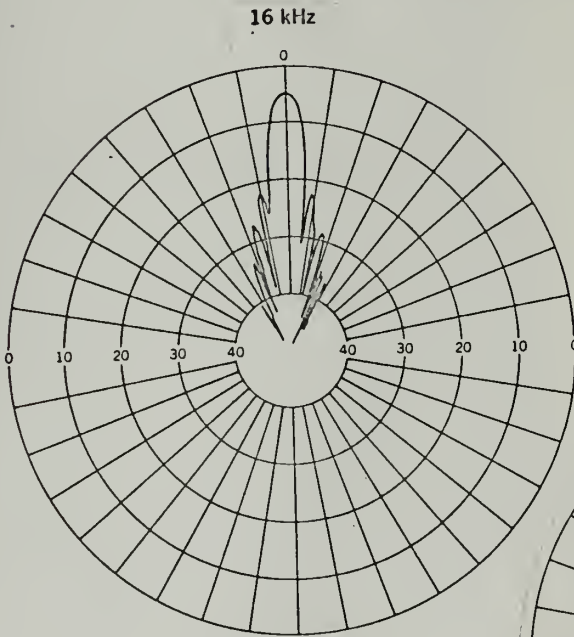
APPENDIX (F)

MODEL 202 TRANSDUCER

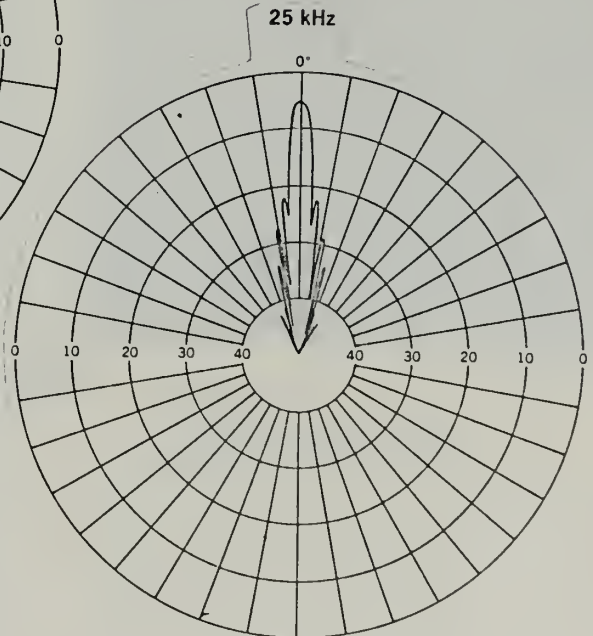
PERFORMANCE CHARACTERISTICS

Operating Band	16 kHz	25 kHz	35 kHz
Directivity Index	29 db	33.4 db	36.5 db
Beam Width	6.5°	4.2°	2.8°
Efficiency	40%	75%	55%
Impedance Parallel Tuned	50 ohms	50 ohms	50 ohms
Receiving Sensitivity	-84 db	-80 db	-84 db
Active Face Diameter	34"	34"	34"
Operating Depth	500 ft.	(1000 ft. optional)	

TRANSMITTING DIRECTIVITY PATTERNS



(Taken from: EDO
Western Corporation
Data Sheet CB-4A)



Thesis

P46173

Pfingstag

Narrow beam echo
sounds.

127252

21 SEP 71
21 SEP 71

DISPLAY
S 9935

Thesis

P46173

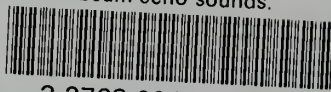
Pfingstag

Narrow beam echo
sounds.

127252

thesP46173

Narrow beam echo sounds.



3 2768 001 97860 4
DUDLEY KNOX LIBRARY